ISSN 8755-6839

SCIENCE OF **TSUNAMI HAZARDS**

Journal of Tsunami Society International

Volume 38 **Number 1** **2019**

FAST EVALUATION OF TSUNAMI WAVES HEIGHTS AROUND KAMCHATKA AND KURIL ISLANDS **1**

Mikhail Lavrentiev[1,2], Konstantin Lysakov[1,2], Andrey Marchuk[3], Konstantin Oblaukhov[2,4], and Mikhail Shadrin[1,2]

[1] Institute of Automation and Electrometry SD RAS, 1 Ac. Koptyug pr., Novosibirsk, 630090 **RUSSIA**
[2] Novosibirsk State University, 1 Pirogov st., Novosibirsk, 630090, **RUSSIA**
[3] Institute of Computational Mathematics and Mathematical Geophysics SD RAS, 6 Ac. Lavrentiev pr., Novosibirsk, 630090, **RUSSIA**

NUMERICAL MODELING OF THE NEVELSK EARTHQUAKE AND TSUNAMI OF 2 AUGUST 2007 **14**

R.Kh. Mazova, N.A. Baranova, I.V. Remizov, T.A Morozovskaia., V.I Melnikov, A.A.Rodin

Nizhny Novgorod State Technical University n.a. R.E. Alekseev, Nizhny Novgorod, ***RUSSIA***

REDUCTION OF THE RISK BY TSUNAMI: EVACUATION PROCESSES IN CHILEAN CITIES DURING THE EARTHQUAKES OF 2010 AND 2015 **30**

Leonel Ramos [1*] - Hitomi Murakami [2]

Department of Urbanism, University of Concepcion, **CHILE**
[2] Yamaguchi University, **JAPAN**

TSUNAMI SOCIETY INTERNATIONAL, 1741 Ala Moana Blvd. #70, Honolulu, HI 96815, USA.

SCIENCE OF TSUNAMI HAZARDS is a CERTIFIED OPEN ACCESS Journal included in the prestigious international academic journal database DOAJ, maintained by the University of Lund in Sweden with the support of the European Union. SCIENCE OF TSUNAMI HAZARDS is also preserved, archived and disseminated by the National Library, The Hague, NETHERLANDS, the Library of Congress, Washington D.C., USA, the Electronic Library of Los Alamos, National Laboratory, New Mexico, USA, the EBSCO Publishing databases and ELSEVIER Publishing in Amsterdam. The vast dissemination gives the journal additional global exposure and readership in 90% of the academic institutions worldwide, including nation-wide access to databases in more than 70 countries.

OBJECTIVE: Tsunami Society International publishes this interdisciplinary journal to increase and disseminate knowledge about tsunamis and their hazards.

DISCLAIMER: Although the articles in SCIENCE OF TSUNAMI HAZARDS have been technically reviewed by peers, Tsunami Society International is not responsible for the veracity of any statement, opinion or consequences.

Submit manuscripts of research papers, notes or letters to the Editor. If a research paper is accepted for publication the author(s) must submit a scan-ready manuscript, a Doc, TeX or a PDF file in the journal format. Issues of the journal are published electronically in PDF format. There is a minimal publication fee for authors who are members of Tsunami Society International for three years and slightly higher for non-members. Tsunami Society International members are notified by e-mail when a new issue is available. Permission to use figures, tables and brief excerpts from this journal in scientific and educational works is granted provided that the source is acknowledged.

Recent and all past journal issues are available at: http://www.TsunamiSociety.org CD-ROMs of past volumes may be purchased by contacting Tsunami Society International at postmaster@tsunamisociety.org Issues of the journal from 1982 thru 2005 are also available in PDF format at the U.S. Los Alamos National Laboratory Library http://epubs.lanl.gov/tsunami/

WWW.TSUNAMISOCIETY.ORG

ISSN 8755-6839

SCIENCE OF TSUNAMI HAZARDS

Journal of Tsunami Society International

Volume 38 Number 1 2019

FAST EVALUATION OF TSUNAMI WAVES HEIGHTS AROUND KAMCHATKA AND KURIL ISLANDS

Mikhail Lavrentiev[1,2], Konstantin Lysakov[1,2], Andrey Marchuk[3], Konstantin Oblaukhov[2,4], and Mikhail Shadrin[1,2]

[1] Institute of Automation and Electrometry SD RAS, 1 Ac. Koptyug pr., Novosibirsk, 630090 Russia
[2] Novosibirsk State University, 1 Pirogov st., Novosibirsk, 630090 Russia
[3] Institute of Computational Mathematics and Mathematical Geophysics SD RAS, 6 Ac. Lavrentiev pr., Novosibirsk, 630090 Russia
[4] "SoftLab-NSK" Ltd, 1 Ac. Koptyug pr., Novosibirsk, 630090 Russia
E-mail addresses: lavrentiev@iae.nsk.su, lysakov@sl.iae.nsk.su, mag@omzg.sscc.ru, oblaukhov@sl.iae.nsk.su, mikesha@sl.iae.nsk.su

ABSTRACT

In this paper, we consider the problem of fast wave heights numerical evaluation of hypothetical tsunami along Pacific coast of Kamchatka Peninsula and the Kuril Islands. We focus on PC-based fast numerical calculation of tsunami wave propagation according to the classical shallow water approximation. Valuable performance gain is achieved by using the advantages of the modern computer architectures, namely the Field Programmable Gates Arrays (FPGAs). The Mac-Cormack finite difference scheme of the second order approximation to solve the shallow water system (Titov V. and Gonzalez F. 1997) has been implemented to the FPGA-based Calculator, specially designed by the authors for this task (Lavrentiev et al., 2017; Lysakov et al., 2018). Numerical tests show that it takes only a few seconds to calculate tsunami wave propagation over approximately 2000x2000 km (3120x2400 knots) water area with about 900 m step gridded bathymetry for the given realistic tsunami wave source. The FPGA calculator was also tested on the exact analytical solution obtained by Marchuk (2017) for model bottom topography.

1. INTRODUCTION

Events of a seismic nature following by catastrophic floods caused by a tsunami wave (the instances of which have increased in the last decades) have an important impact on the population of littoral regions. This paper presents the results of numerical simulation to obtain the distribution of tsunami wave heights using the real bathymetry around Kamchatka Peninsula and Kuril Islands. Characteristics of the source, used for numerical experiments, are close to those of disaster event of March 11, 2011 (The Great East Japan Earthquake). Our goal is to reduce the required time for numerical modeling of tsunami wave propagation by using the proposed hardware-software solution, based of the Field Programmable Gates Array (FPGA). The FPGA-based co-processor, in the sequel referred to as Calculator, is installed on a regular PC.

As is well known, DART (Deep-ocean Assessment and Reporting of Tsunami) buoys, (see https://nctr.pmel.noaa.gov/Dart/) or any other pressure sensor system, like the DONET (Dense Oceanfloor Network system for Earthquakes and Tsunamis) (https://www.jamstec.go.jp/donet/e/), provide measurements of the passing tsunami wave in the real-time mode. So, the measured wave profile is available in real time (even just as the wave is passing over the sensor) through the satellite network channels. Having these measured data, first, it is necessary to recalculate the detected wave profile in terms of the initial sea surface displacement at tsunami source. There are different approaches to do this, see (Hiroaki T. and Yusaku O., 2014; Voronina T., 2016), e.g. We would like to refer also to the "orthogonal decomposition" approach, see (Lavrentiev M., Kuzakov D. et al., 2017; 2018). The corresponding algorithm works very fast estimating the initial water surface displacement at a source in a few seconds with just a regular PC.

Fast calculation of tsunami wave heights distribution along the entire coastal line under study would be really helpful for the local authorities to make a decision about the necessary safety measures to avoid casualties and to reduce economy loss. Calculation of the wave propagation over the given water area is now a rather standard process, based on numerical solution to linear or nonlinear shallow water differential equations. The USA NOAA tsunami warning centers use the so-called MOST (Method Of Splitting Tsunamis) software package, which simulates all tsunami phases – generation, propagation, and inundation of the dry land, see (Titov V. and Gonzalez F. 1997). Here we address the module of MOST software, responsible for calculation of the wave propagation only. As was proved in numerical mathematics, one can trust numerical solution to evolution type system of partial differential equations only if the time step is in a certain relation with the space grid step length. Therefore, calculation with the fine enough computational grid, may require too much time even with an advanced computer. So, one of the possible ways to carry out in time the wave propagation computation from a source up to a shoreline, is nested grids algorithms (Hayashi K. et al., 2015). The second way is using the modern computer architectures like Graphic Processing Unit (GPU) or FPGA microchip.

Presently, most of performance gain is due to the parallel implementation of a given data processing algorithms. Such parallel calculations require the corresponding hardware, namely multi-core CPU clusters (rather expensive within supercomputing units), GPU based hybrid systems, or FPGA microchip based special processors. Using FPGA microchip advantages, we accelerate solution to system of shallow water equations. The achieved performance at regular PC with the proposed Calculator is nearly 250 times faster compared to propagation of the real wave (6 sec against 1600 sec).

The rest of the paper is as follows. We first present a version of shallow water system, used for numerical computations and the description of the Mac-Cormac numerical scheme. Comparison of numerical solution with the analytic one for model bathymetry is also given. In the next section the proposed Calculator – hardware device for code execution acceleration, is briefly described. Then the results of a number of numerical tests, arranged at the real digital bathymetry with 30 arc sec (nearly 900 m) mesh step are presented. We use the initial seabed displacement at tsunami source similar to those of the Great Tohoku Earthquake of 2011. Obtained numerical results are then discussed.

2. MATHEMATICAL STATEMENT OF THE PROBLEM

The referred software package MOST (like many other tools) uses the following equivalent form of a shallow water system (which does not take into account such external forces as sea bed friction, Coriolis force and others), which could be found in (Titov V. and Gonzalez F. 1997):

$$\begin{aligned} &H_t + (uH)_x + (vH)_y = 0, \\ &u_t + uu_x + vu_y + gH_x = gD_x, \\ &v_t + uv_x + vv_y + gH_y = gD_y, \end{aligned} \qquad (1)$$

where $H(x, y, t)=\eta(x, y, t)+D(x, y, t)$ is the entire height of water column, $\eta(x,y,t)$ being the sea surface disturbance (wave height), $D(x,y)$ – depth (which is supposed to be known at all grid points), u and v components of water flow velocity vector, g – acceleration of gravity.

The so-called Mac-Cormack scheme (MacCormack R. and Paullay A., 1972) was used for numerical treatment of the shallow water system (1). The Mac-Cormack algorithm is a direct difference scheme at three-point stencil of a "cross" type. Simulation domain is assumed to be a fixed rectangle (respectively to geographic coordinates), time independent:

$$\Omega((x,y) = \{(x,y): X_1 \le x \le X_2,\ Y_1 \le y \le Y_2,\ X_i,\ Y_j - const\}.$$

The uniform rectangle grid is considered in Ω:

$$\overline{\Omega}\,(x,y) = \{((x_i,y_j): X_1 \le x_i \le X_2,\ Y_1 \le y_j \le Y_2, 0 \le i \le N_x,\ 0 \le j \le N_y\},$$

where $\Delta x = x_{i+1} - x_i$, $\Delta y = y_{i+1} - y_i$ – grid steps with respect to variables x and y, respectively. Consider the partition of the time period for wave propagation:

$$\bar{\gamma} = \left\{ t^n) : 0 \le n \le N_t \right\}$$

$\tau^n = t^{n+1} - t^n$ – time steps. For simplicity, in the sequel we use a uniform step $\tau^n = \tau$, while, in case of necessity, it is not a problem to use the variable time steps. We will use standard notation for the mesh variables Φ at node *(i,j)*, as $\Phi_{ij}^n = \Phi(x_i, y_j, t^n)$.

The shallow water equations (1) at the mesh nodes $\overline{\Omega}$ on the *n*-th time step will be approximated with the help of explicit two-steps Mac-Cormack finite difference scheme of the second order approximation:

1st step:

$$\frac{\widehat{H}_{ij}^{n+1} - H_{ij}^n}{\tau} + \frac{H_{ij}^n u_{ij}^n - H_{i-1j}^n u_{i-1j}^n}{\Delta x} + \frac{H_{ij}^n v_{ij}^n - H_{ij-1}^n v_{ij-1}^n}{\Delta y} = 0,$$

$$\frac{\widehat{u}_{ij}^{n+1} - u_{ij}^n}{\tau} + u_{ij}^n \frac{u_{ij}^n - u_{i-1j}^n}{\Delta x} + v_{ij}^n \frac{u_{ij}^n - u_{ij-1}^n}{\Delta y} + g\frac{\eta_{ij}^n - \eta_{i-1j}^n}{\Delta x} = 0, \qquad (2)$$

$$\frac{\widehat{v}_{ij}^{n+1} - v_{ij}^n}{\tau} + u_{ij}^n \frac{v_{ij}^n - v_{i-1j}^n}{\Delta x} + v_{ij}^n \frac{v_{ij}^n - v_{ij-1}^n}{\Delta y} + g\frac{\eta_{ij}^n - \eta_{ij-1}^n}{\Delta y} = 0.$$

2nd step:

$$\frac{H_{ij}^{n+1} - \left(\widehat{H}_{ij}^{n+1} + H_{ij}^n\right)/2}{\tau/2} + \frac{\widehat{H}_{i+1j}^{n+1}\widehat{u}_{i+1j}^{n+1} - \widehat{H}_{ij}^{n+1}\widehat{u}_{ij}^{n+1}}{\Delta x} + \frac{\widehat{H}_{ij+1}^{n+1}\widehat{v}_{ij+1}^{n+1} - \widehat{H}_{ij}^{n+1}\widehat{v}_{ij}^{n+1}}{\Delta y} = 0,$$

$$\frac{u_{ij}^{n+1} - \left(\widehat{u}_{ij}^{n+1} + u_{ij}^n\right)/2}{\tau/2} + u_{ij}^n \frac{\widehat{u}_{i+1j}^{n+1} - \widehat{u}_{ij}^{n+1}}{\Delta x} + v_{ij}^n \frac{\widehat{u}_{ij+1}^{n+1} - \widehat{u}_{ij}^{n+1}}{\Delta y} + g\frac{\widehat{\eta}_{i+1j}^{n+1} - \widehat{\eta}_{ij}^{n+1}}{\Delta x} = 0, \qquad (3)$$

$$\frac{v_{ij}^{n+1} - \left(\widehat{v}_{ij}^{n+1} + v_{ij}^n\right)/2}{\tau/2} + u_{ij}^n \frac{\widehat{v}_{i+1j}^{n+1} - \widehat{v}_{ij}^{n+1}}{\Delta x} + v_{ij}^n \frac{\widehat{v}_{ij+1}^{n+1} - \widehat{v}_{ij}^{n+1}}{\Delta y} + g\frac{\widehat{\eta}_{ij+1}^{n+1} - \widehat{\eta}_{ij}^{n+1}}{\Delta y} = 0.$$

Usually, the real tsunami wave simulation is performed in a spherical or geodetic coordinate system (λ,φ), where λ is the longitude and φ is the latitude in arc degrees. Accordingly, the following relations are used to calculate the differences Δx and Δy:

$$\Delta x_{ij} = \frac{\pi(\lambda_{i+1} - \lambda_i)}{180^\circ} R_E \cos(\varphi_j),$$

$$\Delta y_{ij} = \frac{\pi(\varphi_{i+1} - \varphi_i)}{180^\circ} R_E,$$

where R_E stands for the Earth radius. This scheme looks similar to the splitting method (with respect to space variables), which is used in the MOST software package. Indeed, in order to calculate the values of the sought functions at grid-point *(i,j,n+1)* the values at 3 points of the previous time step *(i,j,n) (i-1,j,n) (i,j-1,n)* are used during the first half-step in (2), and the values at the points *(i,j,n) (i+1,j,n) (i,j+1,n)* during the

second half-step in (3). However, comparison of the known analytic solutions with the numerically obtained ones show that the proposed attempt to realize the three-points calculation stencil (Mac-Cormack scheme) seems to be preferable compared to the one from the MOST software package (Lavrentiev et al., 2017; Lysakov et al., 2018).

Indeed, precision of the proposed implementation of the Mac-Cormack scheme has been tested by a comparison of the computed solution with the known analytic solutions for the model case of the parabolic bottom topography, see (Marchuk An., 2017). The 1000 * 1000 km littoral area was considered, where the depth increases according to the formula:

$$D(x,y)=10^{-8}\cdot y^2,$$

where the ordinate y means the distance to the coastline. As is observed in Fig. 1, the achieved precision is the same or better, as compared to the MOST software package.

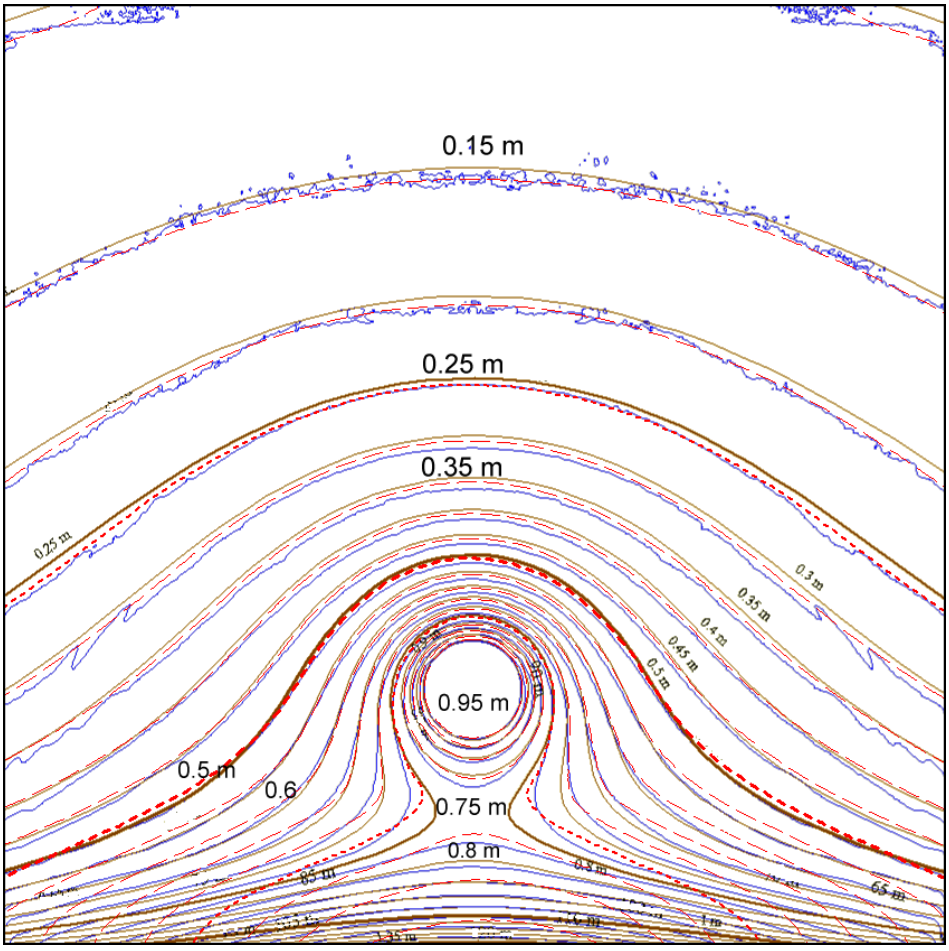

Figure 1. Comparison of the wave height maxima distribution obtained within ray approximation (brown isolines) with results of numerical modelling using FPGA calculator (red isolines) and by the MOST software (blue isolines).

3. FPGA BASED CALCULATOR

Modern Field Programmable Gate Array (FPGA) microchips provide the possibility of parallel implementation of hundreds of thousands of simultaneous computation flows; their internal memory attains tens of megabits. FPGAs are configurable processors, i.e., the same hardware device may serve as a special processor for different tasks, depending on a particular loaded algorithm. This platform makes it possible to construct the computational architecture the most suitable for the implemented algorithms. Moreover, FPGA microchips can be reconfigured an unlimited number of times to solve different problems or change processing algorithm.

According to difference scheme (2)-(3), at each grid-point it is necessary to calculate the values of three grid-functions: H_{ij}^{n+1}, u_{ij}^{n+1}, and v_{ij}^{n+1}. For the FPGA algorithm implementation, the stream processor architecture was proposed. It consists of a certain processor elements (PEs). Such PEs executes a version of a 2-dimension run, a pipeline with a sequential data stream. The auxiliary data for each node required to be stored in memory, are the values of all functions in use at 4 neighbor nodes forming computation stencil. The FPGA architecture makes it possible to use the fast inner memory (BRAM) for implementing such stencil buffer.

The input data flow is a sequential line-by-line inspection of all the grid points. The suggested PE architecture allows either processing several points simultaneously, or connecting in series several PEs to implement several iterations as a single pipeline. This makes it possible to optimize the PE set according to the peculiarities of a given hardware platform. The mathematical operations in (2), (3) of Mac-Cormack difference scheme are implemented as a calculation pipeline, with performance of 1 node treatment at one computer clock cycle.

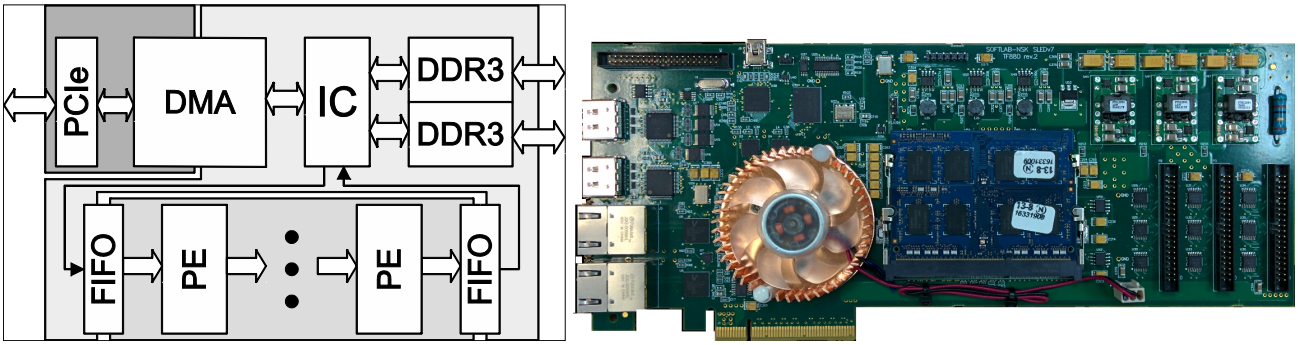

Figure 2. Operation scheme and appearance of the FPGA based Calculator.

Block-scheme of the Calculator and its appearance are given in Fig. 2. In addition to Processing Elements (PE's), which perform calculation in parallel mode, the Calculator has memory controllers DDR3, PCIe controller, and DMA modulus responsible for the direct access to the host computer memory. The Calculator receives the input data from the memory through FIFO (First In, First Out) memory, which makes it possible to adopt the frequency of separate calculation modules tuning it to the particular FPGA microchip as well as the outer memory and interface characteristics. Calculator may contain several PEs, depending on the characteristics of a particular FPGA in use. Block-scheme of the Calculator, based of FPGA microchip Xilinx Virtex-7 VC709, is available in (Lavrentiev et al., 2017; Lysakov et al., 2018).

Let us give some explanations about calculation pipeline realized in this FPGA based Calculator. Recent version contains 16 Processing Elements (PEs). The sequence of tasks is arranged as follows. The first couple of PEs works on calculation of the tsunami flow parameters corresponding to the time layer *n+1*. Both PEs use the digital bathymetry array depth values and wave parameters on the previous time layer only along 3 lines of computational domain which are enough for obtaining values of H_{ij}^{n+1}, u_{ij}^{n+1}, v_{ij}^{n+1} ($i=1,..,N_x$) along the certain line *j* of rectangle grid $\overline{\Omega}$. First PE obtains values on the intermediate time layer *n+1/2*, which are used by the second PE for the almost simultaneous calculating of wave parameters for time layer *n+1*. Then this couple of PEs takes into account wave parameters H_{ij}^{n}, u_{ij}^{n}, v_{ij}^{n} ($i=1,..,N_x$) and the depth along the next line *j+2* of computational domain, where the values for time layer *n+1* along the grid line *j+1* must be calculated. So, line-by-line the first couple of PEs calculates and sends to DMA the wave parameters for time layer *n+1*. When these tsunami parameters have been obtained (with the help of first couple of PEs) for first 3 grid lines of domain, then the second couple of PEs starts calculating wave parameters for time layer *n+2*. After the first 3 lines have been completed by the second couple of PEs the third couple starts to work on the time layer *n+3*, and so on. After completing the time layer *n+1* by the first couple of PEs, it starts processing grid variables for time layer *n+9*. This pipeline cycle continues up to the numerical experiment number of time steps limit. The FPGA calculator simultaneously works on wave parameters at 8 time layers with 3 grid lines delay each.

4. NUMERICAL EXPERIMENTS

Numerical experiments were arranged at the gridded bathymetry around Kamchatka Peninsula and Kuril Islands, visualization of which is presented in Fig.3. This 30 arc sec resolution gridded bathymetry was developed in Bezhaev, Marchuk and Seliverstov (2002) based on the large number of depth soundings provided by “Vulkanolog” vessel. For ocean depth description in far-field areas the segments of global digital bathymetry database developed in (Smith and Sandwell, 1997) have been added. This digital bathymetry and computational grid have the following characteristics:

- Grid size is 3120x2400 points
- Grid steps are 30 arc seconds in both directions (which means approximately 584 and 928 meters, respectively);
- Array covers the area between 144° and 170° E, 41° and 61° N;
- Time step used in computations is equal to 1.0 sec.

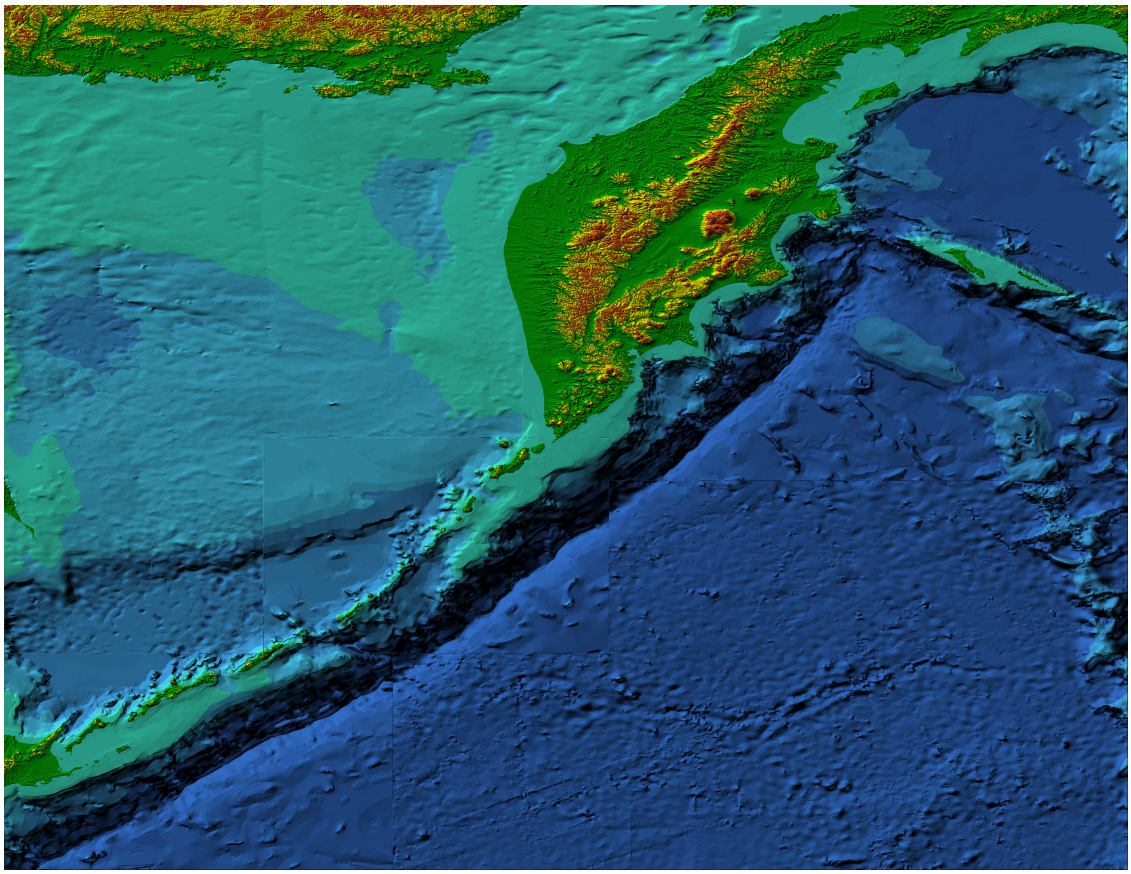

Figure 3. Digital bathymetry of the Russian Far-East Kuril-Kamchatka region.

The FPGA based Calculator with a regular modern PC needs 24 sec to simulate the first 90 minutes of the wave propagation from the dipole-type source. This source looks similar to the unit source used for tsunami forecast by NOAA (Gica E. et al., 2008) but significantly stretched in one direction. The shape and profile of the typical unit source is based on the available geological and geophysical information. Due to this, the typical for subduction zone seabed displacement area for 7.5 M earthquake was approximated by 50x100 km rectangle having maximum water surface elevation as 57 cm. The initial seabed displacement at such a unit source is shown in Fig. 4.

Figure 4. 2D shaded and 3D views of the source used for numerical modeling.

The extended 500 km long model tsunami source was used in numerical experiment. The source size has the same order as 1952 Kamchatka and 2011 Great Tohoku tsunami sources but the maximum initial water surface elevation at source is taken equal to +200 cm. Geographic location of this source is shown in Fig. 5 as two ellipses. The part of source with the initial surface depression is located closer to the coast than the uplift wing. The "real" propagation time for the wave in this case is evaluated as 6000 sec. This includes wave approaching and reflecting off the shore processes.

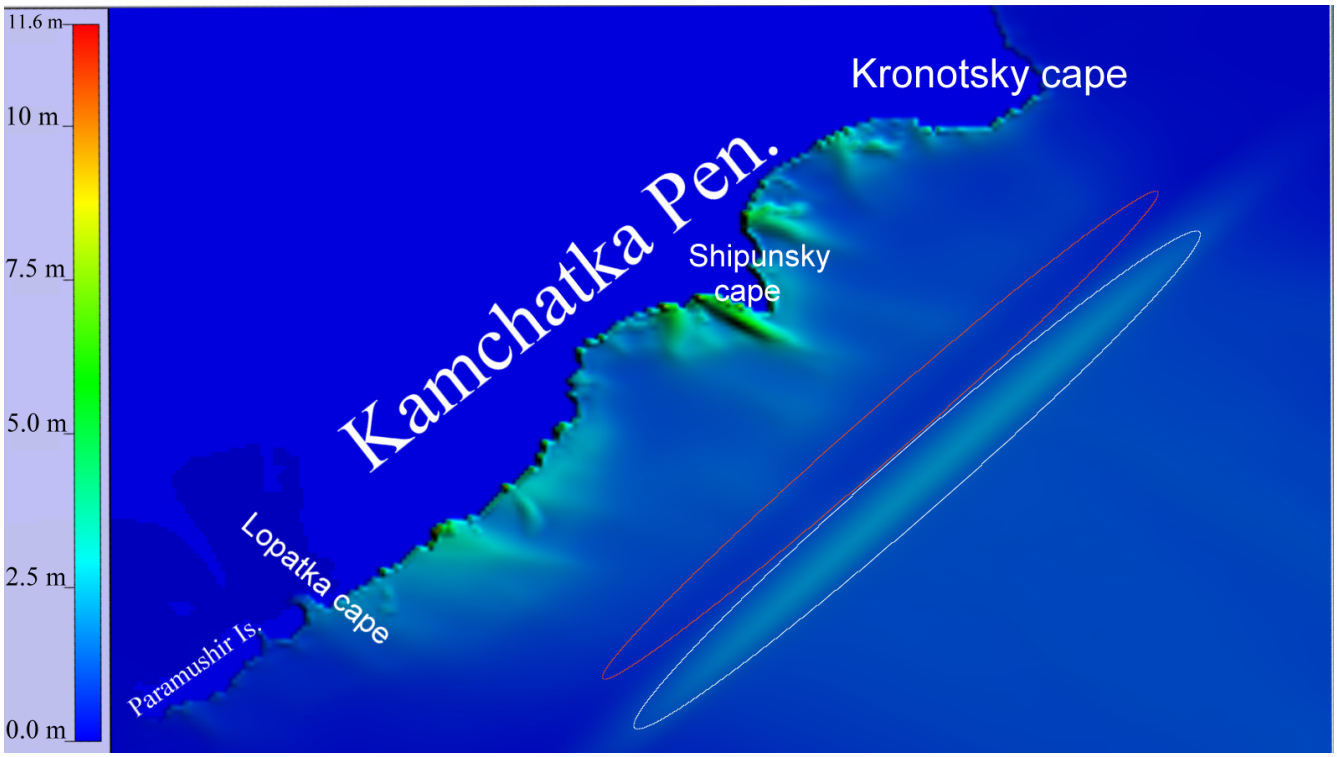

Figure 5. Position of model tsunami source eastward of Kamchatka peninsular and distribution of the wave maxima near the Northern Kuril and Kamchatka coast.

Numerical simulation with the 3120x2400 nodes computational grid shows that the main wave approaches the nearest shore in approximately 1600 sec after the shock. With the proposed FPGA based Calculator, it takes only a few seconds to calculate the maximal height distribution along the entire coastline considered. Namely, it takes 29.95 sec for the Calculator based on Virtex-6 microchip (SLEDv7 printed board), while just 5.98 sec with VC709 microchip. The similar computational experiment was carried out using MOST software. It takes not less than 1.0 sec for calculating each time step on the medium class PC (2.5-3.0 GHz). In the other words, it takes approximately 1800 sec for calculation with the MOST software tsunami propagation up to the nearest coast. So, the performance gain, achieved by the proposed Calculator, is nearly 250 times compared to the MOST software. It means that calculation is executed at least 250 times faster compared to propagation of the real wave (6 sec against 1600 sec).

Figure 6 shows the more detailed FPGA computed distribution of tsunami wave maxima along the North Kurils and Kamchatka shore for the tsunami source under study.

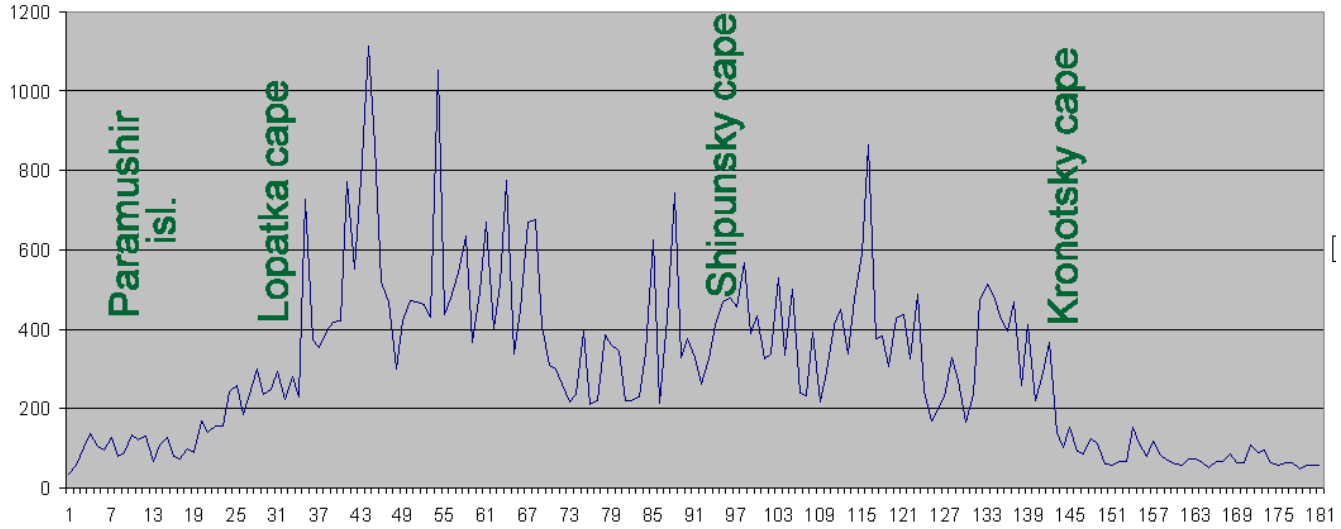

Figure 6. Distribution of tsunami wave maxima (in centimeters) along North Kurils and Kamchatka shore obtained with FPGA based Calculator.

This wave-height distribution shows that for such location of the initial sea surface displacement (Fig. 5) the highest tsunami waves (up to 12 m) are expected at some harbors in the southern part of Kamchatka Peninsula. At the coastline areas, which are not just opposite to the described source, the height of tsunami is significantly lower (100-200 cm only). It is comparable to the maximal vertical displacement at tsunami source. In order to verify numerical results, obtained with the described FPGA based Calculator, the same numerical experiment was carried out using MOST software. Fig. 7 below presents the computed maximal heights of tsunami wave generated by the same extended source, which is shown in Fig. 4.

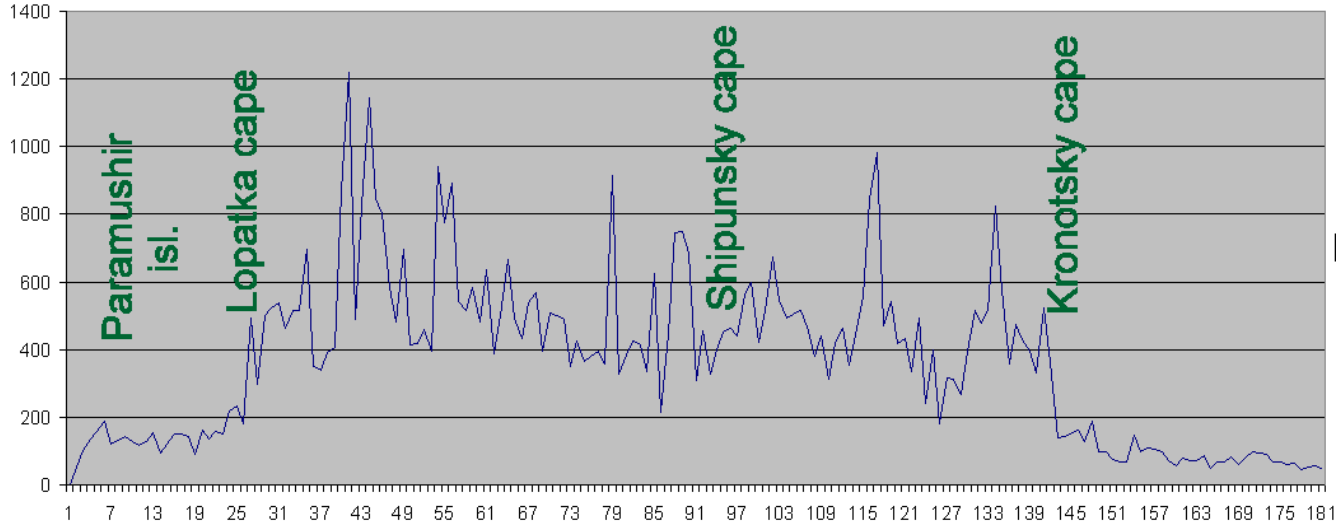

Figure 7. Distribution of tsunami wave maxima along the shore calculated by MOST software.

As is observed from the Fig. 7, the maximum tsunami heights distribution along the North Kurils and Kamchatka coast is similar to the one obtained using FPGA based Calculator. This comparison proves reliability of numerical results obtained with FPGA based Calculator, which can be obtained within few seconds after start of calculation. Let compare this processing time to hours required for computation using MOST software.

Now, let us say few words about the digital bathymetry, used for numerical tests. Usually, the grid step is determined by the available bathymetry databases, accounting for the goals of numerical modeling. These days such grid step, typically about 900 m, is considered too large. However, it depends on the modeling goals. When one needs a detailed evaluation of the expected wave heights along the entire shoreline, it is necessary to carry out numerical modeling with the corresponding fine mesh size in the near-coast regions. It could be done by choosing the properly small grid step in the entire water area. However, the number of computational nodes will increase by 2-3 orders, which results in the necessity of extended computational facilities or, alternatively, in a dramatic increase of the CPU time required for simulation. As for the proposed FPGA-based Tsunami Wave Calculator, the available memory resources dictate the limit of approximately 50 millions for a number of computational nodes.

There is even a more important challenge. Refining a computational grid using interpolation of depth values to 10-20 m resolution will miss the fine details of real bathymetry, which are not reflected in the original 900 m resolution database. Therefore, results of numerical modeling will be rather far from reality in the near shore areas. Natural solution to this problem could be obtained by the nested grids approach, where the resolution depends, roughly speaking, on the distance to the shore. Of course, the fine digital bathymetry in the coastal area is required for obtaining the detailed wave height distribution along the shoreline. A combination of the nested grids approach with the hardware code acceleration (by the use of Graphic Processing Units – GPU) has been tested by the authors simulating tsunami wave propagation at Sanriku coast, see (Hayashi K. et al., 2015).

When the fine digital bathymetry in the coastal area is available, it is not a problem to pass the obtained numerically wave parameters from the original «rough gridded» area to the one with a fine grid. The algorithm in use admits simultaneous computations in several near-coast areas. So, by using just a few of the proposed FPGA based Calculator, PCs gives ability for Tsunami Warning Centers (services) to obtain the robust evaluation of maximal tsunami wave heights along the entire coastal region by the reasonably short time, certainly much less compared to the wave travel time from the source to the coast.

5. DISCUSSION

Having such tool as the designed “Tsunami Wave” Calculator, operating with the regular PC as a co-processor, it is possible to move toward the real-time instrument for the local authorities to evaluate tsunami danger in any particular part of the coast. Indeed, shortly after strong near shore underwater seismic event the magnitude and epicenter location is known. In case the event could be dangerous, special service (municipal, e.g.) can order (and certainly pick up) the time series – tsunami wave profile, measured by

available sensor system (DONET, S-NET, DART buoy, or any other). Rather simple algorithm, see (Lavrentiev M., Kuzakov D. et al., 2017; 2018) will recalculate these data in terms of the initial seabed (sea surface) displacement at tsunami source just in a few seconds. Then, using the Calculator, any expert is able to calculate an approximation of the expected wave height distribution along the valuably long part of the coast. As the computation takes less then a minute, several scenarios (differ from each other by small shifts of the initial displacement area) could be processed. Short calculation time gives possibility to use longer wave time series for reconstruction tsunami source which must improve the final height prediction. This would provide a solid ground for decision makers for evacuation measures.

After development and testing of a number of the real time algorithms, covering the entire process, namely: automated order of tsunami wave profile from the sensor network, automated accounting of the tidal component, wave profile recalculation in terms of the initial sea bed displacement at tsunami source, generation of adaptive digital bathymetry, calculation of tsunami wave propagation, inundation mapping, it will be possible to create the real time decision support software for tsunami warning services.

6. CONCLUSION

As a step toward the real-time tsunami danger evaluation, the FPGA-based specialized Calculator has been designed and tested. It uses FPGA microchip, which dramatically accelerates numerical modeling of tsunami wave propagation. Calculation of the tsunami wave propagation from the hypothetic source up to the Kuril-Kamchatka shoreline in the 3120x2400 knots computational domain takes only a few seconds. So, the wave height distribution along the coast can be determined almost immediately after restoration of the initial water surface displacement at the tsunami source area. As was shown earlier, the precision of numerical results is the same then using the MOST software, the official tool of NOAA (USA) tsunami warning centers. These results show the possibility of tsunami danger forecast in the real-time mode. The authors will propose soon a version of software which uses nested grids approach to obtain characteristics of a tsunami wave along the detailed shoreline.

7. ACKNOWLEDGEMENTS

This study was supported, in part, by the project 0319-2018-0010 IV.36.1.4. Investigation and development of methods and technologies for construction of integrated software-hardware systems to modeling and control of dynamical systems for data processing and presenting, registration number AAAA-A17-117062110016-4, Institute of Automation and Electrometry SB RAS.

REFERENCES

DART® (Deep-ocean Assessment and Reporting of Tsunamis) [Electronic resource]: https://nctr.pmel.noaa.gov/Dart/

DONET (Dense Oceanfloor Network System for Earthquakes and Tsunamis) [Electronic resource]: https://www.jamstec.go.jp/donet/e/

Gica E., Spillane M.C., Titov V.V., Chamberlin C.D., Newman J.C. Development of the Forecast Propagation Database for NOAA's Short-Term Inundation Forecast for Tsunamis (SIFT), *NOAA Technical Memorandum OAR PMEL-139, Pacific Marine Environmental Laboratory*, Seattle, WA, March 2008.

Hayashi K., Vazhenin A.P., Marchuk An.G. Trans-Boundary Realization of the Nested-Grid Method for Tsunami Propagation Modeling. *Proceedings of the Twenty-fifth (2015) International Ocean and Polar Engineering Conference.* Kona, Big Island, Hawaii, USA, June 21-26, V. 3, International Society of Offshore and Polar Engineers (ISOPE), pp. 741-747. 2015.

Hiroaki T., Yusaku O. Review on Near-Field Tsunami Forecasting from Offshore Tsunami Data and Onshore GNSS Data for Tsunami Early Warning. *Journal of Disaster Research* V. 9 No. 3, pp. 339-357. 2014.

Lavrentiev M.M., Kuzakov D., Romanenko A.A., Vazhenin A.P. Determination of Initial Tsunami Wave Shape at Sea Surface. *Oceans'17 MTS/IEEE, Aberdeen, June 19-22*, 2017

Lavrentiev M.M., Kuzakov D., Marchuk An.G. Determination of Initial Sea Surface Displacement at Tsunami Source by a Part of Wave Profile. *Oceans'18 MTS/IEEE, Kobe, Japan, May 28-31*, 2018.

Lavrentiev M.M., Romanenko A.A., Oblaukhov K.K., Marchuk An.G., Lysakov K.F., Shadrin M.Yu. FPGA Based Solution for Fast Tsunami Wave Propagation Modeling. *The 27th International Ocean and Polar Engineering Conference, 2017, 25-30 June, San Francisco, California, USA* pp 924-929. 2017.

Lysakov K.F., Lavrentiev M.M., Oblaukhov K.K., Marchuk An.G., Shadrin M.Yu. FPGA-based Modelling of the Tsunami Wave Propagation at South Japan Water Area. *Oceans'18 MTS/IEEE, Kobe, Japan, May 28-31*, 2018.

MacCormack R.W., Paullay A.J. Computational Efficiency Achieved by Time Splitting of Finite-Difference Operators. *AIAA paper*. – 1972. – No. 72-154.

Marchuk An.G. Benchmark solutions for tsunami wave fronts and rays. Part 2: Parabolic bottom topography. *SCIENCE OF TSUNAMI HAZARDS*, Vol. 36, No 2, 2017, pp. 70-85.

Marchuk An.G., Bezhaev A.Yu. and Seliverstov N.I. New gridded digital bathymetry for the Kuril-Kamchatka region. *Recent Advances in Marine Science and Technology' 2002, USA, Honolulu, Narendra K. Saxena Editor, PACON International, P.O/ Box 11568, Honolulu, Hawaii 96828 USA*, 2002. (http://nippon.zaidan.info/seikabutsu/2002/00223/contents/044.htm)

Smith W.H.F. and Sandwell D. Global seafloor topography from satellite altimetry and ship depth soundings. *Science* 1997, 277: pp. 1956-1962.

Titov V.V., Gonzalez F.I. Implementation and testing of the method of splitting tsunami (MOST) model. *NOAA Technical Memorandum ERL PMEL-112*, 1997

Voronina T.A. Recovering a tsunami source and designing an observational system based on an *r*-solution method. *Numerical Analysis and Applications* V. 9, No. 4. pp. 267–276. 2016.

ISSN 8755-6839

SCIENCE OF **TSUNAMI HAZARDS**

Journal of Tsunami Society International

Volume 38 **Number 1** **2019**

NUMERICAL MODELING OF THE NEVELSK EARTHQUAKE AND TSUNAMI OF 2 AUGUST 2007

R.Kh. Mazova, N.A. Baranova, I.V. Remizov, T.A Morozovskaia., V.I Melnikov, A.A.Rodin
Nizhny Novgorod State Technical University n.a. R.E. Alekseev, Nizhny Novgorod, ***RUSSIA***

ABSTRACT

The anomalous tsunamigenic earthquake, which occurred on August 2, 2007 at 02.37 GMT in the Tatar Strait, near the western coast of Sakhalin Island (Nevel'sk earthquake), is examined. Though the magnitude of the main shock was M=6.2, the tsunami waves generated by this earthquake were abnormally large, reaching heights of more than 3 meters at some points of the coast. Generally, earthquakes of similar magnitudes do not cause significant tsunami waves but only waves, which are very weak. Also unusual about this event was the distribution of maximum wave heights along the entire west coast of Sakhalin Island, from Chekhov to Korsakov, which were proceeded by recessions of coastal water. The present study presents the numerical simulation of this earthquake and of the tsunami it generated. Two scenarios of possible seismic sources are being considered, the dynamics of which can explain the unusual distributions of tsunami wave heights along the coast.

***Key words*:** earthquake source, anomalous tsunami waves, numerical simulation

INTRODUCTION

Earthquakes occurring in the Kuril- Kamchatka zone mainly generate tsunamis in the Far Eastern region of Russia. For the period from 1737 to 1983 more than 60 tsunami events were observed or recorded on the Pacific coast of the country. According to historical and instrumental data, the coasts of Sakhalin Island are rarely struck by tsunamis [1-3]. The greatest danger for Sakhalin is tsunamis generated from seismic sources in the Sea of Japan. The most famous of these events is the Moneron tsunami of 5 September 1971, when a wave height of up to 2 m was recorded on the south coast of Sakhalin. Tsunami waves, which occur in the seismically active zone of Kuril-Kamchatka and reach the shores of Sakhalin, are usually weakened due to the attenuation effect of the Kuril ridge. An unexpected event was the generation of an "anomalous" tsunami of 2 August 2007 (at 02.37 GMT) in the area of the Tatar Strait, 60 km off Yuzhno-Sakhalinsk. This moderate earthquake with magnitude Mt = 6.2, generated tsunami waves on the west coast of Sakhalin that reached up to 3 meters in height [4,5].

1. Features of the Nevel'sk earthquake and tsunami 02.08.2007.

As noted in [4], the heights of tsunami waves on the coast, which were generated by the Nevel'sk earthquake on 2 August, 2007, indicate that the magnitude of this earthquake could not have been 6.2 as reported, but was significantly more. Also, in the scientific literature [4,5] it is noted that the tsunami in the Nevel'sk region followed immediately after the main shock, and began with a strong withdrawal of the water along the coast. Anomalous for this earthquake was also the rise of some parts of the coastal zone, the so-called "benches", both in the Nevel'sk region and in other parts of the coast. A significant feature of this earthquake is the ambiguity in data in the determination of the earthquake's epicenter, apparently due to the occurrence of several aftershocks comparable in strength to the main shock [4,5]. According to the US Geological Survey [https://earthquake.usgs.gov], the epicenter of the earthquake had coordinates 47.116 ° N 141.798 ° E (2007-08-02 02:37:42 (UTC)), and was located at a depth of 5 km, while according to the network of autonomous digital seismic stations (DAT) of the SF of the GS of RAS [http:// www.globalcmt.org] the coordinates of the epicenter were given as: 46.829 ° N, 141.756 ° E [4] (Table 6.1), with focal depth of 10.6 km.

One of the characteristic features of the Nevel'sk earthquake was that the tsunami that was generated began with a withdrawal of water in many parts of the coast (see Fig.1). It is well known that when a tsunami begins with rundown of water, the subsequent waves could have anomalously high run-up [6,7]. In addition, the character of the tsunami waves that struck the coast was very unusual: the run-up and rundown of the first waves at various points did not have any regularity, which makes it difficult to explain. The maximum heights of the waves on the coast were distributed very unevenly, not diminishing, and often, increasing, with increasing distance from the epicenter of the earthquake along the coast [8,9]. In the same case, when the seismic source was quite long, and the hypocenter was shallow the existing coastal and shelf faults (identified or not identified at the time of the earthquake) can give additional heterogeneous displacements, which in turn significantly affect the formation of tsunami waves. As known, the generation of a tsunami wave depends on the character and character and dynamics of bottom displacements in the zone of the earthquake source, or more

precisely, on the initial bottom displacements. It is also known that when calculating the generation of tsunami waves, seismic data are used to determine the orientation of fractures in the source, then the model of the seismic source is refined, the energy of this earthquake is recalculated into the possible energy of tsunami and then, using various models of numerical simulation of tsunami wave propagation from source to coastal zone, an assessment is made of possible run-up of tsunami waves onto the coast [8,9]. In such computations, there is always the question of the adequacy of the seismic source model, and this is especially true for the tsunami formed by the source located in the near-field zone, i.e. at a distance of the order of the wavelength from the source to the nearest coast. At the same time, the obtained results directly depend on the choice of the model for determining the seismic source of the earthquake. Therefore, it was very important to determine the correct location of the seismic source, as well as to understand the possibility of the existence of crustal faults passing through this source. At the same time, an important characteristic of this work was the availability of data on detailed field studies of the west coast of Sakhalin Island from Yablochnoye point to Gornozavodsk one, conducted by staff members of IMGG FEB RAS. As noted in [5], of the "identified and fairly reliably mapped on land directly to the east of the city of Nevel'sk, there is a relatively long (about 40 km) sub-meridional fault of the type of thrust or uplift-thrust".

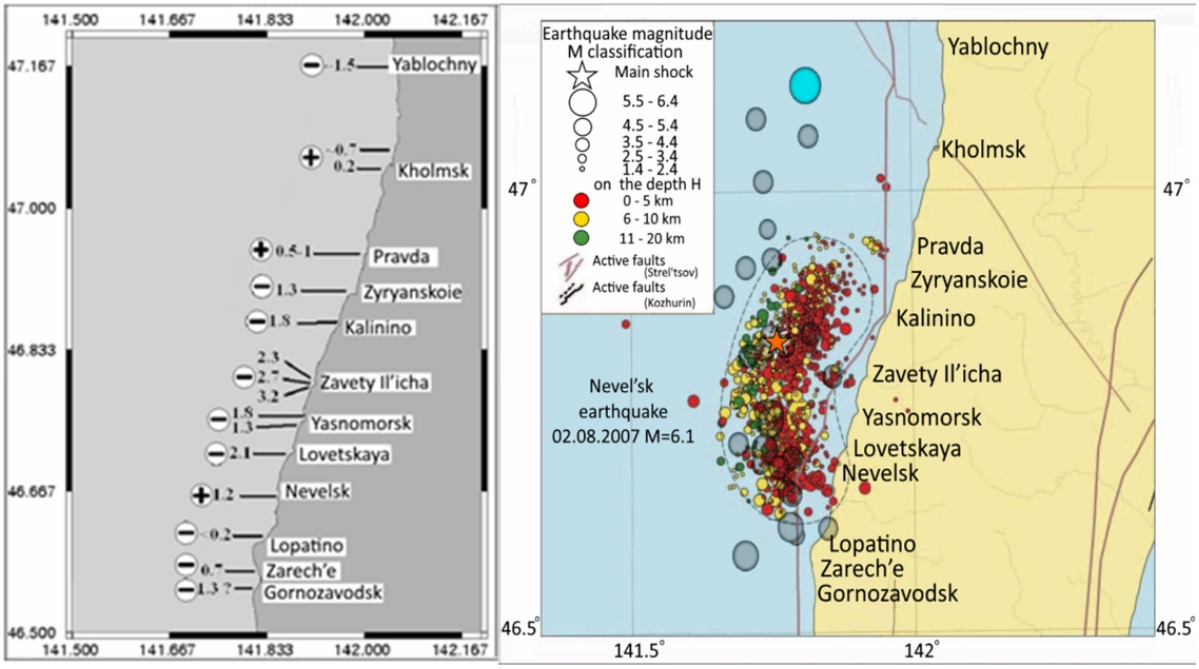

a) **b)**

Fig. 1. a) Character of tsunami wave run-up on the west coast of Sakhalin island at Nevel'sk earthquake (02.08.2007, M=6.2); (+) first elevation wave at run-up on the beach, (-) first depression wave at run-up on the beach [4,5]; b) earthquake main shock epicenter map (orange star) and its aftershocks (encountered by grey dashed curve) – the data are from [4]; grey circles of aftershocks and blue ring of epicenter – the data are from USA Geological Service [https://earthquake.usgs.gov].

2. *The mechanism of the Nevelsk earthquake of 02.08.2007 and the choice of scenarios for a seismic source*

In Fig.1b above, it is clearly seen that the aftershock zone covers the entire shelf zone, partially entering the dry shore, in the area surveyed by the coast. This zone has a lengthy character, which indicates the possible lengthy character of the earthquake source.

In Fig. 2 the map of active geotectonic faults [10] and the relief map of Sakhalin Island [4] are presented. The model seismic sources used for numerical modeling of the Nevel'sk earthquake and tsunami are also schematically shown here.

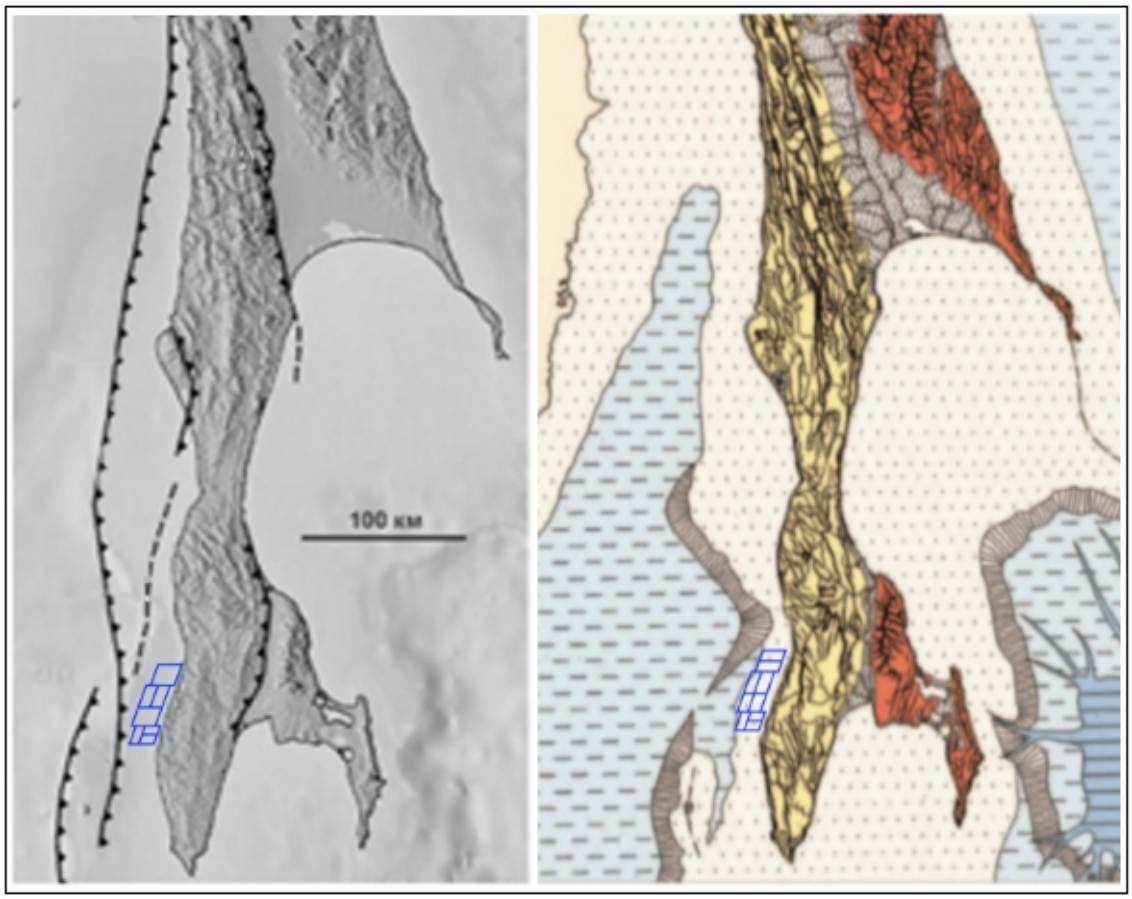

a) b)

Fig. 2 Model representation of computational source for Scenario 1 and Scenario 2 at maps: a) active faults of Sakhalin island [10]; b) relief of Sakhalin island [4]; blue lines – schematical representation of earthquake sources for two scenarios.

As noted in [4,5], the location of the aftershocks "coincides well with the route of the West-Sakhalin fault and almost all of the aftershocks are located on the western wing of this fault." An analysis of

the factors cited in [4,5,10-12], (see Fig.2a, b) suggests that the seismic source consisted of a series of key blocks [8], the implementation of which at different times led to such an unusual distribution of run-up heights on the coast and to such a strange pattern of distribution of waves on the coast (see Fig.1a).

Also, it should be noted that a similar character of tsunami wave height distribution, in addition to the specified implementation of movements in a multi-block seismic source, can be determined by waveguide effects along the coastal zone, i.e. captured waves. In this case, the energy of the waves generated by an underwater seismic source located on the shelf is captured by the shelf and the wave, which is subsequently reflected from the coast, then from the edge of the shelf (as in a waveguide), spreads along the coast, slowly attenuating [13]. In this case, the wave process is oscillatory in character: the form of the wave field is determined by the decay of the wave into separate oscillating trains (corresponding to each mode of the captured wave) with different speeds of movement: high-frequency components propagate ahead and lower-frequency components coming only later [14]. When they are superposed, a complex pattern of interference arises, leading to a non-monotonic change in the height of the run-up along the coastline. However, in this paper, the effect of such a process on the distribution of waves along the coastal zone will not be considered.

3. Numerical simulation of the Nevel'sk earthquake and tsunami 02.08.2007.

To study the earthquake of August 2, 2007, in the Tatar Strait, we analyzed the field data obtained from the survey of the western coast of Sakhalin Island [4,5], and analyzed the possible location of the seismic source. Based on the analysis performed, the choice of optimal variants of seismic source dynamics was made, numerical simulation of tsunami wave generation and propagation up to 5-meter isobaths for the water area ($138^0 \div 146^0$ E, $45^0 \div 55^0$ N) was made, with a calculated grid, including 480x599 points.

In this work, a number of calculation options with different implementation of the movements in the source were considered. The choice of options was determined by coastal survey data. It is well known (see, for example, [9]) that the sign of the displacement shift in the center determines the sign of the run-up phase for sources located in the near-field zone, i.e. at a distance of the order of the wavelength. Since we had data on the character of the run-up of tsunami waves from the coastal section from Yablochny to Gornozavodsky points, then the rundown or run-up of the waves at specific points can determine the character of movements in the part of the source that is oriented to this part of the coast. Therefore, the analysis of possible movements of blocks in the source was carried out by selecting the speeds of movement and adjusting the magnitudes of the displacements of a particular block (see, for example, [9]).

Of all the options considered, two Scenarios were selected, the results of which most correlate with the results of field studies of the coast of the western part of Sakhalin, conducted by staff of IMGIG FEB RAS [4]. For numerical simulation of a tsunami, a seismic source was chosen, located at a distance of 2 to 7 km from the coast (depending on the Scenario and on the location of the block),

whose width were 19 km, and 50 km long. For the first Scenario, the source consisted of 7 blocks (see Fig.3a), for the second one - of 9 blocks (see Fig.3b). For Scenario 1, the number of blocks in the seismic source was determined primarily by the character of the bottom bathymetry, and for Scenario 2, by the co-seismic displacements from [4,16,17].

In Table 1, data on the sequence of movement of blocks in the source when implementing Scenario 1 are presented.

Table 1

Block number	1	2	3	4	5	6	7
Shift value (m)	0.6	1	-1	-1	1	-1	-0.6
Start time (sec)	0	20	20	0	0	0	20
Stop time (sec)	10	60	40	10	20	30	30

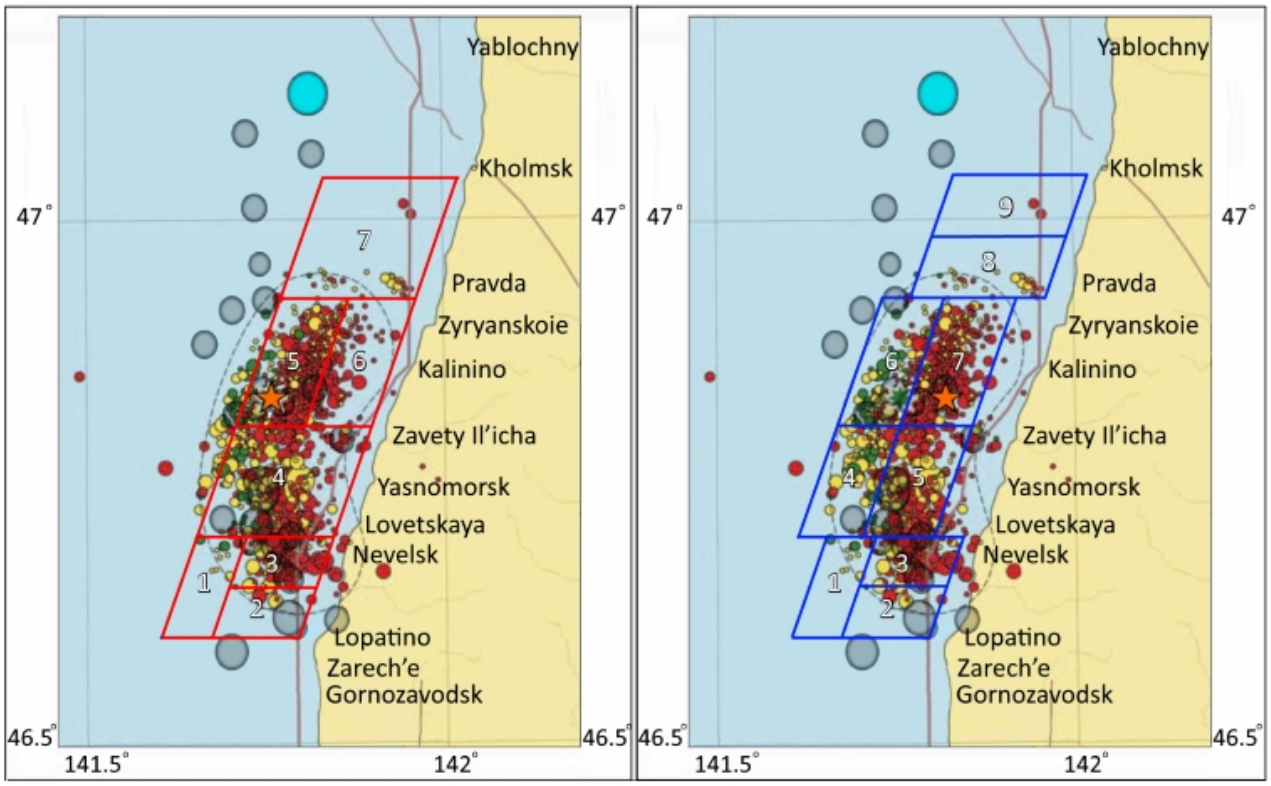

a) **b)**

Fig. 3. Schematic representation of model seismic block sources a) (red contour) for computation on Scenario 1; b) (blue contour) – on Scenario 2. Location of earthquake epicenter for Scenario 1 is determined on data of net of autonomous digital seismic stations (DAT) SF GS RAS [4,5]; for Scenario 2 location of earthquake epicenters is determined on data by Kim Ch.U. (IMGiG Far-East Branch of RAS) [4].

In the framework of nonlinear shallow water equations (see, e.g., [9,13]), numerical simulation of tsunami wave generation by this seismic source, propagation of these waves over the computational area was carried out and maximum wave values were estimated for a number of coastal points (Fig.1a). The simulation was carried out with a time step of 1s, with checking for convergence and stability of the numerical scheme [15]. The results of numerical simulation of the generation and propagation of tsunami waves for Scenario 1 are presented in Fig. 4 and Fig. 5. It is clearly seen that the wave field from such a source is substantially determined by the bottom topography. Thus, the wave front extending towards the continental slope has a well-defined elongated shape, which is caused by faster wave propagation to the underwater depression area, up to 800 m deep. At the same time, the wave front approaching Sakhalin coast is flatter. In addition, there is a predominant propagation of the wave front in the southwestern direction of the Sakhalin coast, while the wave reaches the more northern points of the coast in a longer period of time (Fig.5). This may be due to the greater width of the shelf zone to the north.

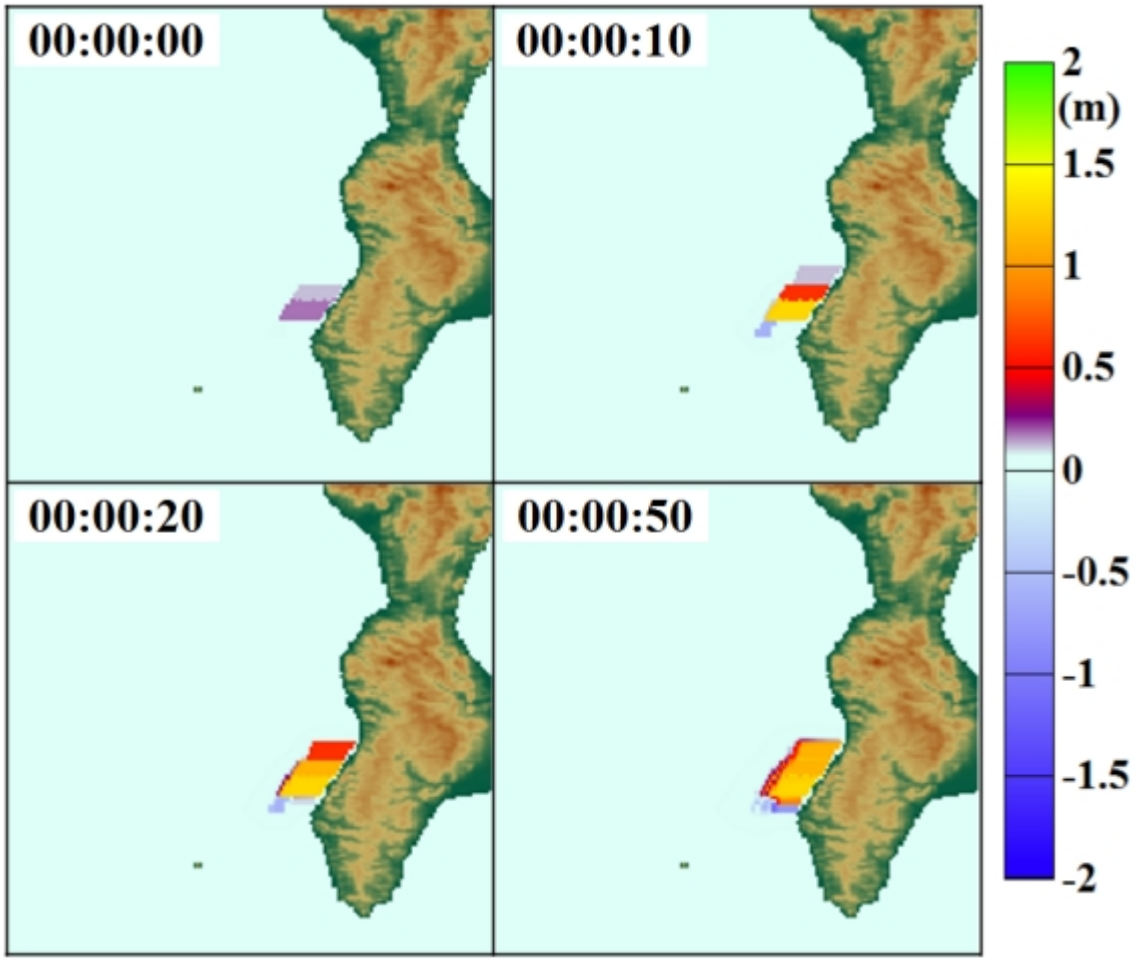

Fig. 4. Formation of tsunami source under implementation of Scenario 1.

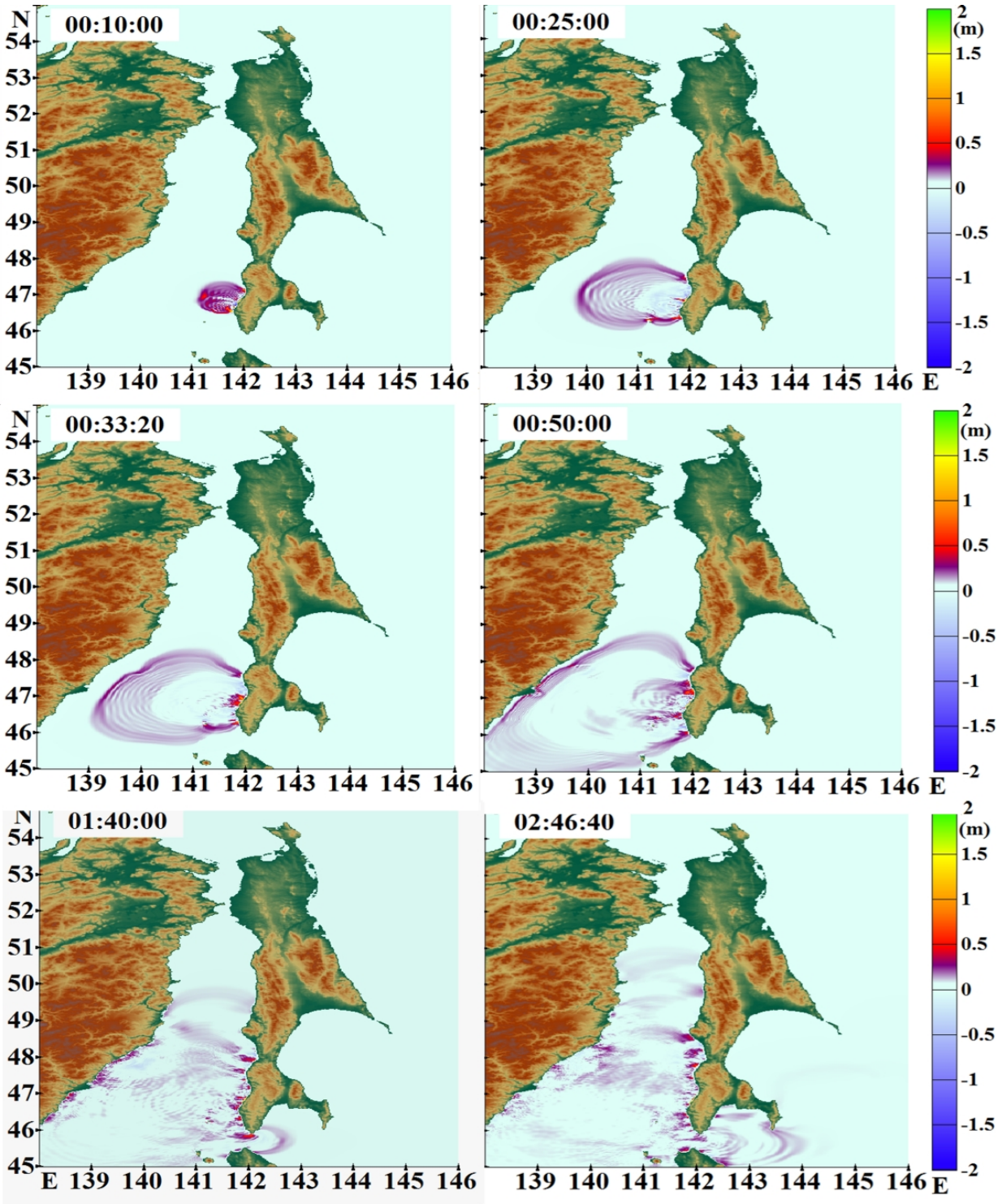

Fig. 5. Propagation of tsunami wave on computational basin at implementation of Scenario 1.

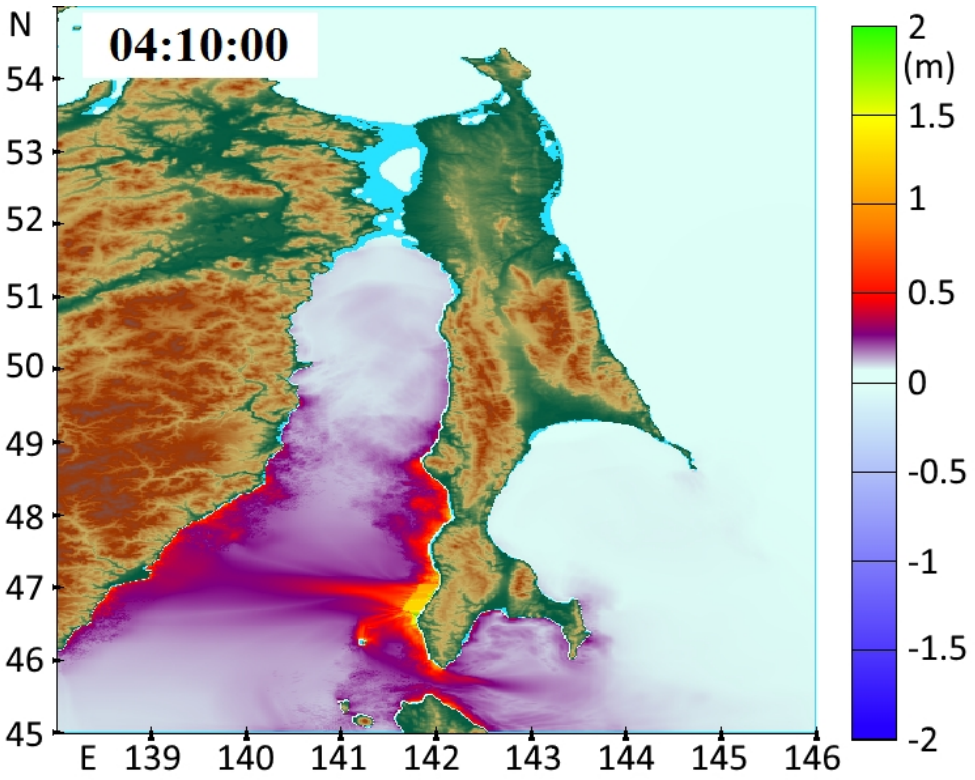

Fig. 6. Maximum wave height distribution in the computational basin (Scenario 1).

Figure 6 presents a picture of the distribution of maximum wave heights in the water area. Its detailed analysis allows us to estimate the effect of possible movements in a seismic source and justify the use of a multi-block key model for calculating the generation.

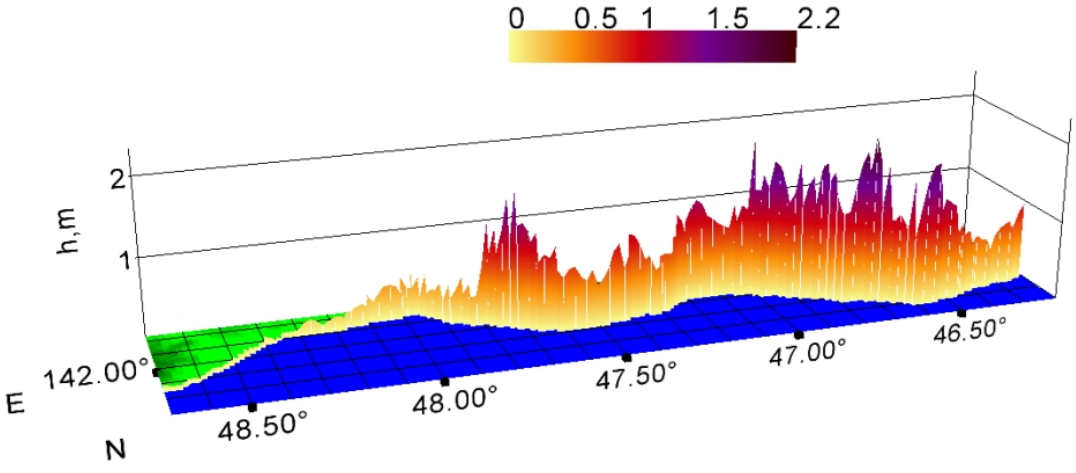

Fig. 7. 3D histogram of maximum tsunami wave height distribution (Scenario 1).

Fig. 7 shows a three-dimensional histogram of the distribution of the maximum heights of tsunamis along the western coast of Sakhalin Island, obtained by computation according to Scenario 1.

It is clearly seen that the highest heights of run-up are in the range from 46.7^0 to 47^0 N, which is consistent with the data shown in Fig.1a. It can be seen that the maximum heights reaching 2.0 m are alternated by heights ranging from 0.3-0.5 m.

For the second computation, a seismic source was used, a schematic view of which is shown in Fig. 3b. When modeling Scenario 2, data from [4,16,17] were used, where it was proposed to apply the one- dimensional distribution of the co-seismic displacements of the earth's surface, obtained using the Japanese ALOS satellite, "which were fixed in a narrow coastal zone less than 10 km wide and about 30 km from the village Lopatino to the village Kalinino" [4,16,17]. The division of the deformation zone into 2 extended sections: the northern section and the southern section, comparable to the corresponding aftershocks with M = 6.2 and M = 5.8, allowed us to present the seismic source in the following form (Fig. 8) and set the dynamics of the key blocks in the source represented in Table 2.

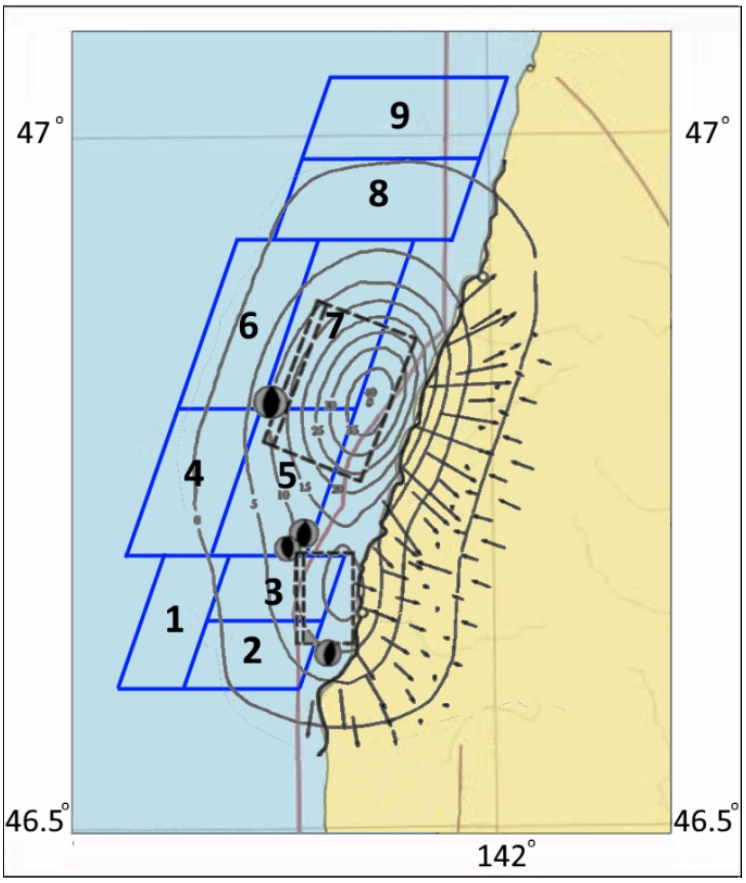

Fig. 8. Schematic representation of model seismic block source (blue contour) for Scenario 2; grey curves are the co seismic shifts from works [4,16,17].

Table 2

Number of case	Block Number	1	2	3	4	5	6	7	8	9
1	Vertical shift (m)	0.5	0.3	-0.4	1.0	-1.5	1.8	-0.8	0.15	-0.15
	Start time (s)	20	20	0	40	30	20	0	50	50
	Stop time (s)	30	40	20	50	40	50	20	70	70
2	Vertical shift (m)					1.8		1.2		0.2
	Start time (s)					40		20		70
	Stop time (s)					60		40		90

In Fig. 9, the generation process of the tsunami source during the implementation of Scenario 2 is shown. Unlike Scenario 1, the beginning of the movement of the blocks corresponding to two sections of the deformation zones (see Fig. 8) can be seen in Fig. 9 (left upper panel). Further aftershock movement to the south and north was approximated by the movement of blocks in the earthquake source (Table 2), which can be seen on the upper right panel of Fig. 9. Such a complex implementation of the dynamics of a seismic source noticeably changed the structure of the wave field in the tsunami source (see Fig. 9, bottom panels).

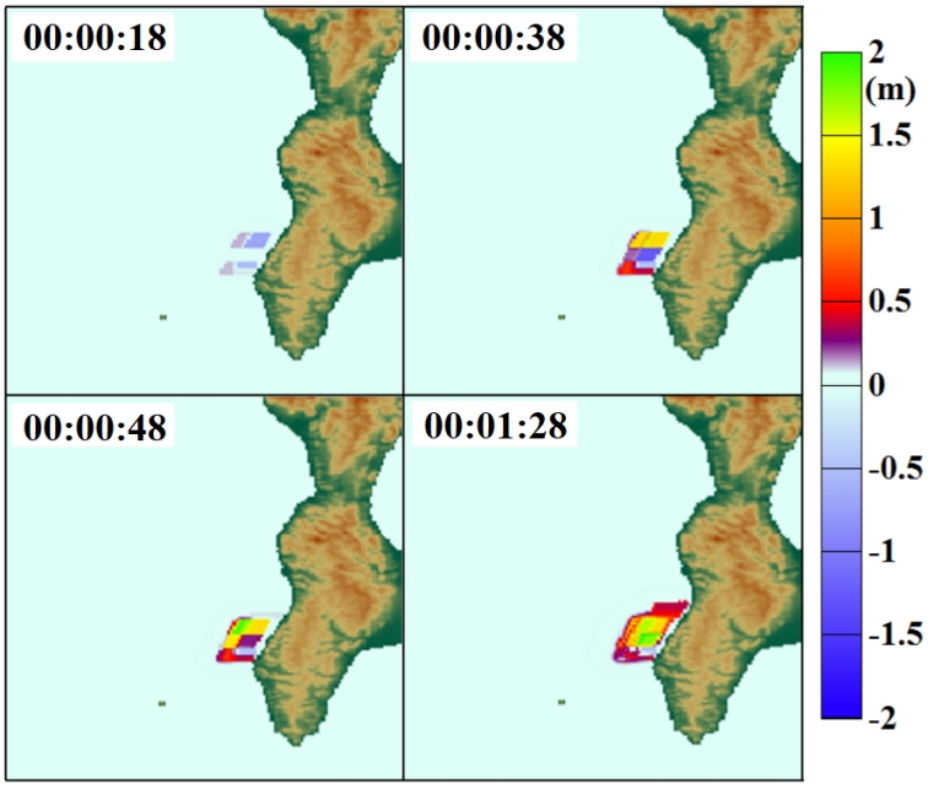

Fig. 9. Formation of tsunami source under implementation of Scenario 2.

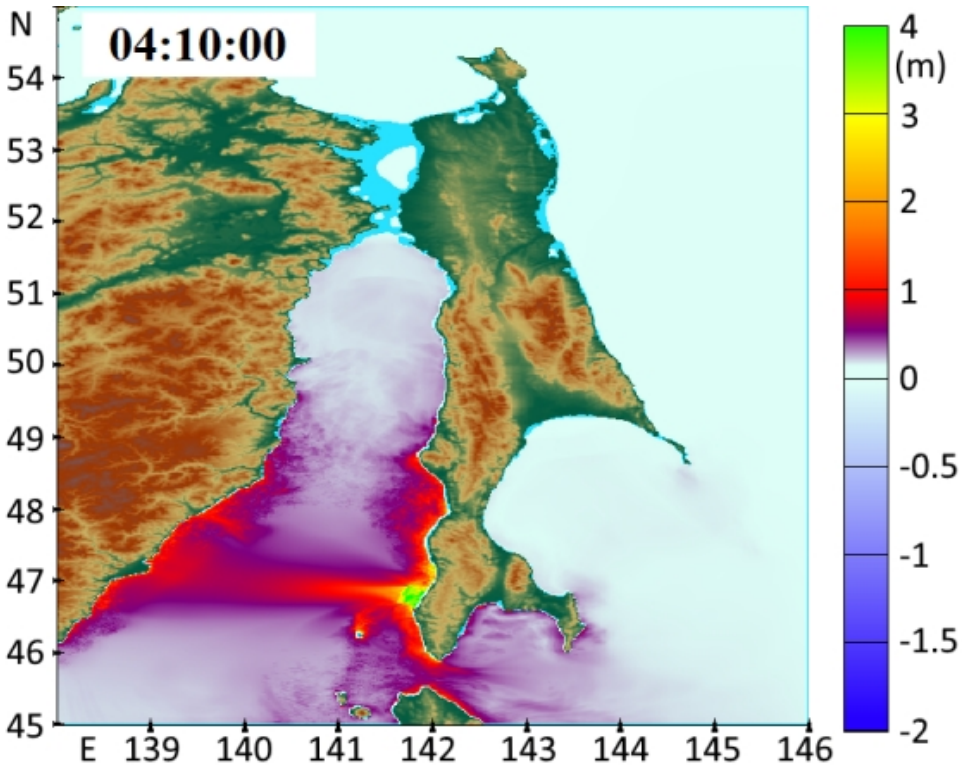

Fig.10. Maximum wave height distribution in the computational basin (Scenario 2).

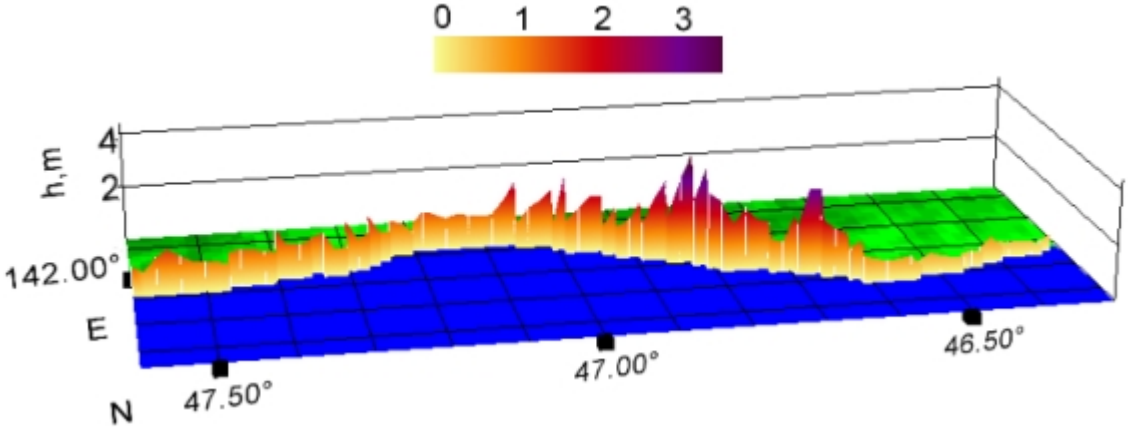

Fig. 11. 3D histogram of maximum tsunami wave height distribution (Scenario 2).

Fig. 10 shows the distribution of maximum wave heights, which is most pronounced along the entire western coast of Sakhalin Island and along the central continental part, which may be due to the peculiarities of the dynamics of this source (Table 2). At the 3d histogram for this scenario, pronounced peaks of heights up to 3.5 m in its central part are observed, alternating with weak rises of water up to 40 cm (Fig.11).

4. ***Comparison of computational with empirical data and data of other authors***

The results of comparison of the obtained computations with empirical data and computations of other authors are shown in Fig. 12 and Table 3. It is clearly seen that the computation data for Scenario 1 (Fig.12a) are weakly consistent with the real data (Fig. 12d), being close to the empirical data only in a limited number of points. This can be explained by the fact that the dynamics of the blocks in the source was determined primarily by the character of the bottom bathymetry. However, the factors described in [4,5,10-12] are rather contradictory, which apparently, did not allow to set the correct dynamics of blocks in the source in Scenario 1.

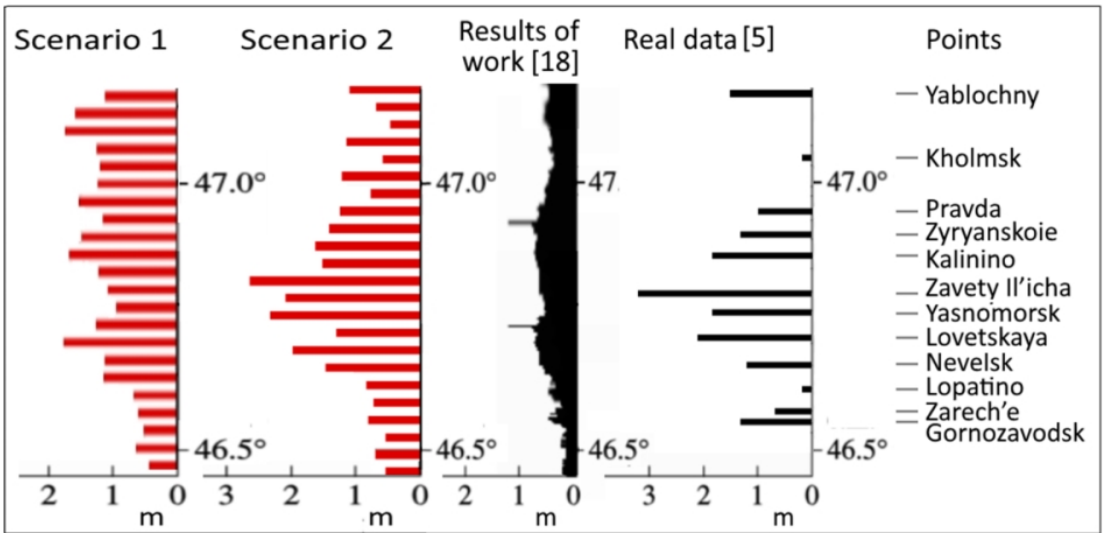

a) b) c) d)

Fig. 12. Comparison of computational and empirical results: a) computation on Scenario 1; b) computation on Scenario 2; c) results from [18-20]; d) real date [4,5].

In Scenario 2, data on the one-dimensional distribution of the co-seismic displacements of the earth's surface [4,16,17] were used (see Fig. 8). It can be seen (Fig. 12b) that the histogram of the distribution of maximum wave heights is closer to the empirical data (see Fig. 12d).

The data from [4,5], which presents the coastal survey results for each item, the results of numerical simulation [21], and the results obtained in calculations for two Scenarios (Scenario 1 and 2) were summarized in Table 3 (column 1, 2, and 3, 4, respectively).

It can be seen that for Znarech'e, Zyryanskoie, Lovetskaya, Pravda the calculated and observed values are close to one other, and a number of calculated data for the maximum run-up heights for points Gornozavodsk, Zavety Il'icha, Kalinino, Yablochny are somewhat underestimated. It is important to note that the calculated data were obtained on a 5-meter isobath, and it is necessary to take into account the gain for the wave height when converting from the shelf zone to the dry shore.

As a result, the calculated wave heights with data obtained on a 5-meter isobath, when recalculated to the coastal zone, may be more consistent with empirical data. At the same time, in such points as Lopatino, Nevel'sk, Yasnomorsk, Kholmsk the estimated heights obtained from Scenario 2 are too high, relative to empirical data. Since in numerical simulations, a multi-block seismic source was preferred, and waveguide effects along the coastal zone, i.e. the captured waves (see above) are possible, these overestimated values of the heights are due to the neglect of these effects.

Table 3

№	Name points	Real data [5] (m)	Numerical modeling [21] (m)	Numerical modeling Scenario 1 (m)	Numerical modeling Scenario 2 (m)
		1	2	3	4
1	Gornozavodsk	1.3	1.4	2	0.9
2	Zarech'e	0.7	1.28	0.8	0.7
3	Lopatino	0.2	-	0.8	0,8
4	Nevelsk	1.2	1.6	1.2	1,6
5	Lovetskaya	2.1	3.15	1.8	2.1
6	Yasnomorsk	1,8	-	1.6	2.3
7	Zavety Il'icha	3.2	3.47	1.8	2.6
8	Kalinino	1.8	1.69	1.0	1.5
9	Zyryanskoie	1.3	-	1.3	1.4
10	Pravda	1	1.67	2	1,2
11	Kholmsk	0.2	1.13	1.1	0,5
12	Yablochny	1.5	0.95	1.3	1.1

5. CONCLUSIONS

Based on this study, one of the conclusions that can be made is that the assumption that the character of the run-up height distribution of the tsunami that hit the coast of Sakhalin after the submarine earthquake of August 2, 2007, depends to a large extent on the specifics of the dynamics, including the underwater seismic source, which determines not only the magnitude of run-up, but also the run-up phase. However, to clarify the computations, it is necessary to take into account the co-seismic displacements of the earth's surface in the coastal zone along the west coast of Sakhalin, and it is also assumed that the waveguide effects along the coastal zone are necessary.

ACKNOWLEDGEMENTS

This work was supported by the grant of the President of the Russian Federation No. NSh-2685.2018.5.

REFERENCES

Murty T.S., Seismic Sea Waves Tsunami, Fisheries Res.Board of Canada, Ottawa, Canada, 1977.

2. Shchetnikov N.A. Tsunami at the coast of Sakhalin and Kuril islands on tide-gauge data 1952-1968 (, Far-East Branch of USSR Acad.of Sci. Press, Vladivostok, USSR, 1990).

3. Soloviev S.L., Go Ch.N. Tsunami catalogue at the west coast of the Pacific Ocean (Nauka Press, Moscow, USSR, 1974).

4. Levin B.V., Tikhonov I.N., Kaistrenko V.M., Kim Ch.U., Sasorova E.V. et al., Nevel'sk earthquake and tsunami 2 August 2007, Sakhalin Island (Yanus Press, Moscow, Russia, 2009).

5. Kaistrenko V.M. et al. Manifestation of Nevel'sk tsunami 2 August 2007 at Tatar strait coast, in Nevel'sk earthquake and tsunami 2 August 2007. Sakhalin island (Eds.: Levin B.V. and Tikhonov I.N., Yanus-K Press, Moscow, Russia, 2009), pp.136-140.

6. Mazova R.Kh, Pelinovsky E.N. The increasing of tsunami run-up height with negative leading wave// In Abstr.Book of Int. Work-shop on Long-Wave Run-up, Catalina Isl., California, USA, August 1990, p.1

7. R. Kh.Mazova, S.L Soloviev. On influence of sign of leading tsunami wave on runup height on the coast // Sci.Tsunami Hazards v.12, p.25-31, 1994.

8. Lobkovsky L.I. Geodynamics of spreading and subduction zones and two-level plate dynamics (Nauka Press, Moscow, USSR, 1988).

9. Lobkovsky L., Garagash I., Baranov B., Mazova R., Baranova N., Modeling Features of Both the Rupture Process and the Local Tsunami Wave Field from the 2011 Tohoku Earthquake, Pure Appl. Geophys. (2017). V.174, p. 3919-3938, doi:10.1007/s00024-017-1539-5 (March 2017) pp.1-20.

10. Mel'nikov O.A. Structure and dynamics of Hokkaido-Sakhalin folded region (Nauka Press, Moscow, USSR, 1987).

11. Lomtev V.L., Nikiforov S.P., Kim Ch.U. Tectonic aspects of core seismicity of Sakhalin, Traqnsact. of Far-East Branch of Russian Acad.of Sci. No.4, p.64-71, 2007.

12. Lomtev V.L., Gurinov M.G. Tectonic conditions of Nevel'sk (02.08.2007, M ~ 6.1) earthquake, Pacific Ocean Geology (2009). V.28, No.5, p.44-53. ISSN 0207-4028.

13. Pelinovsky E.N. Tsunami wave hydrodynamics, (Published by Institute of Applied Physics, Russian Academy of Sciences, Nizhny Novgorod, Russia, 1996).

14. Vol'tsinger N.E., Klevanny K.A., Pelinovsky E.N. Long-wave hydrodynamics of the coastal zone, Gidrometeoizdat, Leningrad, USSR, 1989.

15. Sielecki A. & Wurtele M., 1970, The numerical integration of the nonlinear shallow water equations with sloping boundaries, *Journal of Computational Physics* **6**, 219-236.

16. Vasilenko N.F., Prytkov A.S. Coseismic deformations of the Earth surface in result of Nevel'sk earthquake 2 August 2007. in: Nevel'sk earthquake and tsunami 2 August 2007. Sakhalin island (Eds.: Levin B.V. and Tikhonov I.N., Yanus-K Press, Moscow, Russia, 2009), pp.140-142

17. Vasilenko N.F., Prytkov A.S., Kim Ch.U., Takahashi H. Coseismic deformations of the Earth surface in result of Nevel'sk earthquake 2 August 2007. Pacific Ocean Geology, 2009, v.28, No.5, pp.16-21.

18. Zaitsev A.I., Kovalev D.P., Kurkin A.A. et al. Nevel'sk tsunami 2 August 2007: instrumental data and numerical simulation. Doklady 2008, v.421, No.2, pp.249-252.

19.Zaitsev A.I., Kovalev D.P., Levin B.V., Chernov A.G., Kurkin A.A., Pelinovsky E.N., Yalciner A. The tsunami on Sakhalin on August 2, 2007: mareograph evidence and numerical simulation // Russian Journal of Pacific Geology. 2009. V. 3. No. 5. P. 437-442.

20. Kurkin A.A., Pelinovsky E.N., Choi B.H., Lee J.S. A comparative estimation of the tsunami hazard for the Russian coast of the sea of Japan based on numerical simulation // Oceanology. 2004. V. 44. No. 2. P. 163-172.

21. Zolotukhin D.E., Khramushin V.N. Numerical simulation of propagation of tsunami from the source of Nevel'sk earthquake, in: Nevel'sk earthquake and tsunami 2 August 2007. Sakhalin island (Eds.: Levin B.V. and Tikhonov I.N., Yanus-K Press, Moscow, Russia, 2009), p.143-144.

ISSN 8755-6839

SCIENCE OF TSUNAMI HAZARDS

Journal of Tsunami Society International

Volume 38 Number 1 2019

REDUCTION OF THE RISK BY TSUNAMI: EVACUATION PROCESSES IN CHILEAN CITIES DURING THE EARTHQUAKES OF 2010 AND 2015

Leonel Ramos [1*] - Hitomi Murakami [2]

[1] Professor, Arq, Department of Urbanism, University of Concepcion, Chile.
[2] Professor, Dr. Engr, Yamaguchi University, Japan.
*Corresponding author lramos@udec

ABSTRACT

Tsunamis have always affected Chilean coastal communities, causing great loss of lives and property, and pose a permanent threat to their inhabitants. The Sumatra tsunami in 2004 took hundreds of thousands human lives along the Indian Ocean; similarly, the Chile 2010 and Japan 2011 tsunamis caused great land devastation, though less lives were lost. The Chilean case is of special interest since tsunamis have struck consistently during the last decade, which demands higher social resilience and increased effectiveness in mitigation measures to reduce local and national risk. This research presents a study of the tsunami evacuation processes carried out by the inhabitants during the earthquakes of 2010 and 2015 in the Biobío region, applying a statistical methodology to understand the behavior of the population within a diverse urban and territorial context, with plain and hilly areas. A total of 251 surveys were conducted with inhabitants affected by the tsunamis, to assess the evacuation processes, considering starting time, means of transport, the use of automobiles, traffic jams, and the quality of evacuation routes and safe zones. The objective of the study is to quantify these evacuation processes in an urban context, to prospect possible improvements in the future planning and design of coastal cities.

Keywords: *Tsunami, earthquakes, behavior, evacuation route, safety zones, traffic jams, hazard zones*

1. Introduction

This research presents a study of the tsunami evacuation processes in the cities of Talcahuano and Dichato during the 2010 Maule earthquake, and for the 2015 Coquimbo earthquake; both disasters produced human losses and major material damages on the south-central and northern Chilean coasts; in addition, tsunami warnings led to the evacuation of a significant number of inhabitants from the risk zones to the highlands of the hills along the country's coast in search for shelter.

The 2010 Maule earthquake 8.8 (Mw) occurred at 3:34:08 local time (UTC-3), on Saturday February 27, and triggered a tsunami that affected large parts of the central coast of Chile. The tsunami caused extensive damage in the cities of Talcahuano (Fig. 1) and Dichato; however, the loss of life was very low due to the timely evacuation process performed by the population. The 2015 Coquimbo earthquake occurred at 19:54:31 local time (UTC -3) on Wednesday, September 16, 2015, reaching a magnitude of 8.4 Mw. The epicentre was located 37 kilometres northwest of Los Vilos and 37 kilometres southwest of Canela Baja, in the region of Coquimbo, northern Chile. It was vastly perceived along the country, and also in some areas of Argentina, Uruguay and Brazil. This is the largest event recorded since the 2010 Maule earthquake, and the third largest since May 22, 1960, surpassing the magnitude of the event that occurred off the coast of Pisagua-Iquique on April 1, 2014. The Hydrographic and Oceanographic Service of the Chilean Navy (SHOA) issued a tsunami alarm for the entire Chilean coastal border and almost one million people were orderly and timely evacuated to the security zones. The alarm spread to the shores of the Pacific Ocean abroad, including Peru, Ecuador and Hawaii.

The main objective of the study is to analyze the behavior of the population during the tsunami evacuation process in the earthquakes of 2010 and 2015, considering the time taken to evacuate the hazard zones after the earthquake, the geographical conditions, to determine the main means of transport for evacuation, the start time of the evacuation, the time and distance of the evacuation, the quality of evacuation routes and safe zones, and problems with car traffic and the roads. Furthermore, comparing both experiences will allow to define the strengths and weaknesses as experienced by people during the evacuation process, considering the differences between geographical areas, as well as behaviors that may endanger people and affect the normal evacuation procedure.

2. Research methods and overview of data sources

The main research method used for this paper was the application of 251 surveys to people that were caught in tsunami flood areas during the 27F, 2010 Maule earthquake and the 2015 Coquimbo earthquake. The surveys were applied in different areas (Fig. 1), defined by the morphological characteristics of the territory (flat areas and areas with nearby hills), and by the type of urban land use (residential, industrial, etc.). To facilitate contact with the affected communities, the municipalities of Talcahuano and Tomé collaborated in contacting local leaders to support the implementation of the surveys in each of their community centres.

The sorting and analysis of the results were performed through simple statistics using spreadsheets and crossing information between the different selected areas. The start time of evacuation, evacuation

routes and safe locations were marked using Geographic Information System (GIS) maps, according to information provided by people and duly recorded in the surveys.

To enrich the analysis, specific comparisons were made with the evacuation process performed during the 2011 tsunami in Tohoku region, Japan.

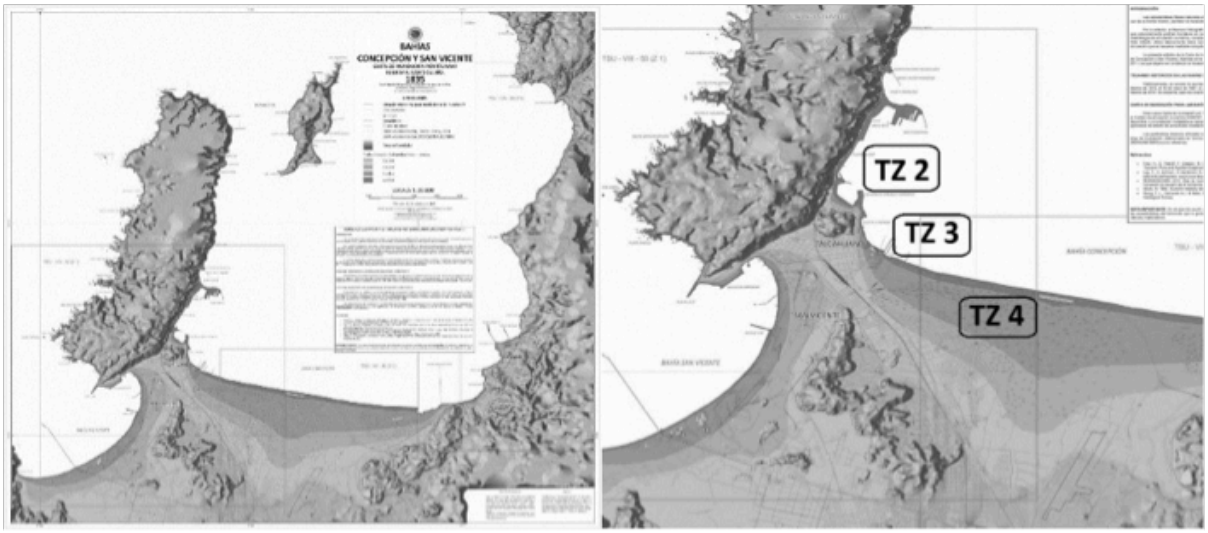

Fig. 1 Study area. Left, Tsunami flood maps of Talcahuano published by SHOA, Chile, based on the historical tsunami events. Right, detail of the area.

3. Earthquake of 2010 and cities affected by the tsunami in Chile

Table 1 shows characteristics and damage conditions in the cities of Talcahuano and Dichato, hit by the 2010 earthquake. The 2010 Maule earthquake (8.8 Mw) occurred at 3:34:08 local time (UTC-3), on Saturday February 27t, and triggered a tsunami which affected large parts of the central coast of the country. The tsunami caused extensive damage in the cities of Talcahuano and Dichato; however, the loss of life was very low due to the timely evacuation process performed by the population. Damage caused by the 2010 tsunami in the cities of Talcahuano and Dichato was very high (Table 1), affecting 26.6% and 65% of the urban area, respectively, and destroying more than 8900 homes. In the case of the 2015 Coquimbo earthquake (8.4 Mw), which occurred on Wednesday, September 16 at 19:54:31 local time (UTC -3), after the activation of the tsunami alarm the population of the cities of Talcahuano and Dichato began the evacuation to the safer higher areas; finally, the waves reached the coast with a height of 1.2 meters, causing minor damage.

Table 1 Cities affected by the tsunami and damage conditions. Developed by author. Source of data: Biobío Region Coastal Border Reconstruction Plan; PRBC18, Master Plan for Dichato and Talcahuano, Government of Chile, 2011. Reconstruction Plan for 27F Earthquake and Tsunami, Government of Chile, August 2010. Statistics of the legal medical service for the 2010 Earthquake, Government of Chile, 2010.

	Talcahuano 2010 8.8 Mw	**Dichato 2010** 8.8 Mw
Population	163.626 people	3.488 people
Extension of urban area	40,3 km²	1,22 km²
Tsunami affected area	10,72 km²	0,803 km²
Houses destroyed by tsunami	7.636	1.343
Tsunami victims	**3**	**16**

4. Questionnaire on tsunami evacuation for the 2010 Maule earthquake

4.1 Geographical conditions of survey area and time to start evacuation

To elucidate tsunami evacuation behaviors in the 2010 Maule earthquake in Chile, a questionnaire survey was conducted in December 2013 for the severely affected city of Talcahuano and the Dichato district of Tomé city, with students of the University of Concepcion participating as interviewers. The survey areas are DCH (Dichato), TZ2 (Talcahuano Central), TZ3 (El Morro), and TZ4 (Salinas). Altogether 193 cases of data were collected. The survey results for: means of tsunami warning, means of transport for evacuation, evacuation routes and conditions; are examined here.

An official tsunami warning was not issued for this earthquake. According to the hearing survey from the disaster management section of Talcahuano municipal office, by the author (H. M.) in 2012, there was a notice from ONEMI that there was no risk of tsunami and that information was broadcast via a local radio station. In the hearing survey at the Dichato temporary housing village on the same occasion, local people and community leaders confirmed the same conditions. Fig. 2 shows tsunami alarm conditions. Overall, 56% of respondents reported that the tsunami alarm did not exist, while 25% said they got some alarm information from neighbors or family.

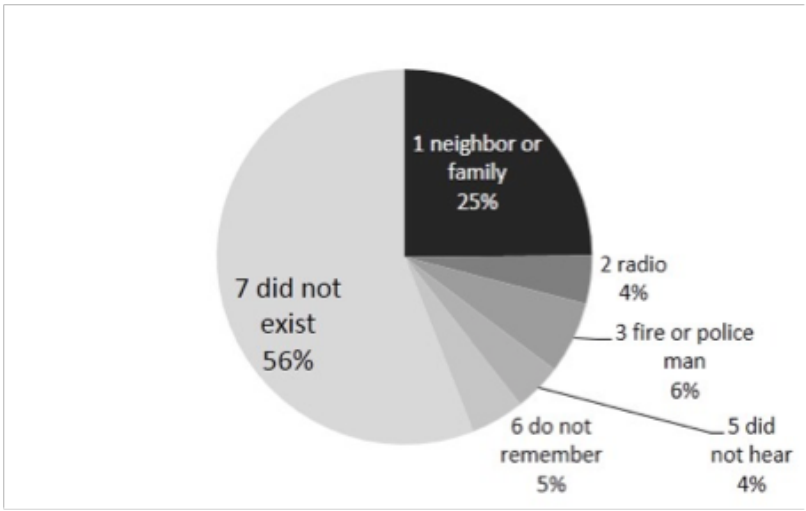

Fig. 2 Tsunami alarm in Biobío (Q3, n=193)

Fig. 3 shows the time taken to start evacuation for each survey zone. Overall, half of respondents started evacuation during the shaking or immediately after the earthquake. Still, 14% of respondents did not, or could not evacuate, and seem to have stayed on the upper floors of apartments or houses. Evacuation was faster in Dichato, and TZ3 El Morro, while it was slower and more respondents did not evacuate in TZ Talcahuano Central. Fig. 4 shows actions taken before starting to evacuate (MR: multiple response) in relation to disabilities. The percentage of those starting evacuation immediately is higher (61%) for those cases with no disability followed by those cases with little disability in walking, and then by those cases of vision or hearing disability. Family teaching of tsunami evacuation prior to the F27 event tends to make people evacuate quicker (Fig. 5), so that it seems to be a primary and basic requirement to promote a quick start for evacuation.

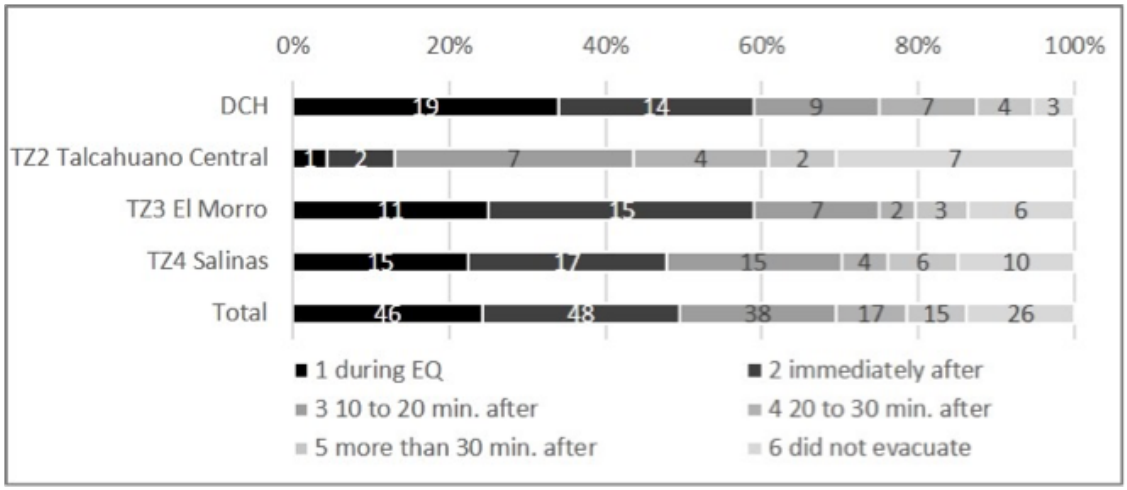

Fig. 3 Time taken to evacuate vs. survey zones (Q5, n=190)

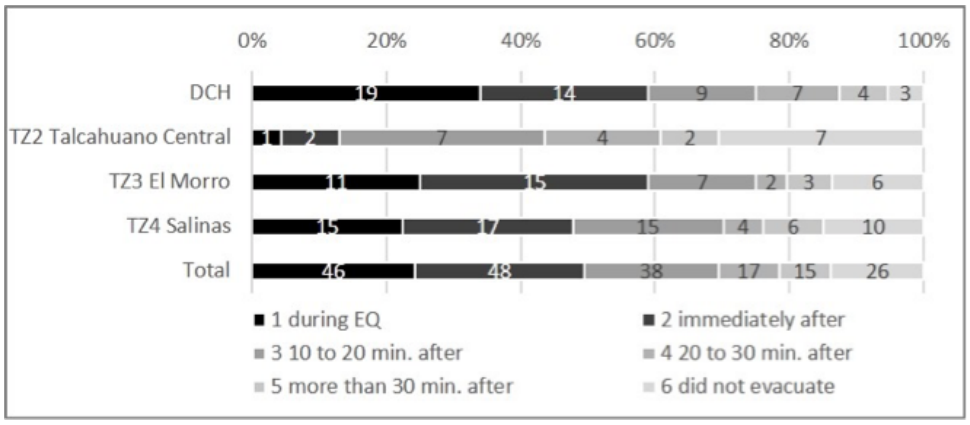

Fig. 4 Actions taken before evacuation vs. disability (MR: multiple response, n=160)

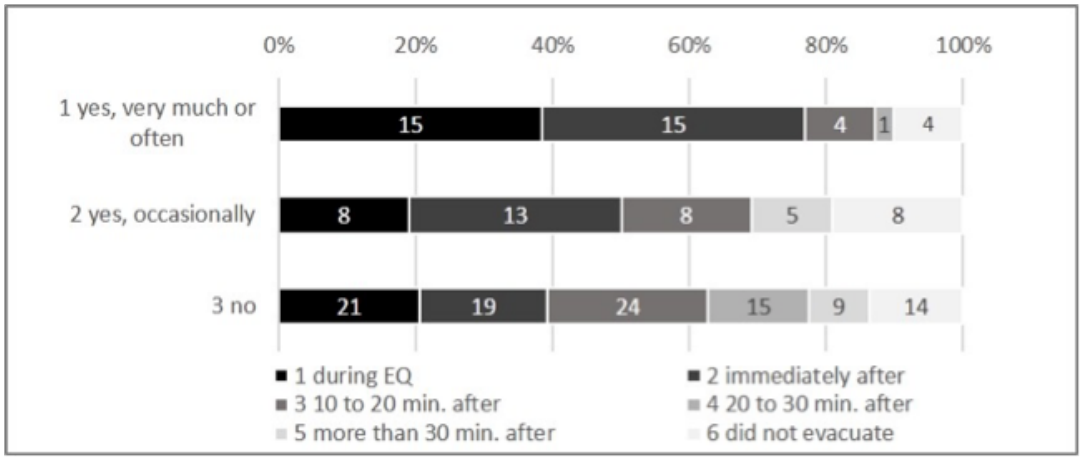

Fig. 5 Q20 Family teaching of tsunami evacuation prior to 27F event and Q5 time to start evacuation (n=183) Pvalue =0.003<0.01

4.2 Transport means for evacuation

Fig. 6 and Fig. 7 show the topography of Talcahuano and Dichato with evacuation routes marked. In Talcahuano, evacuation distances are short (mostly less than 500m) in Zones 2 and 3, and are much longer in Zone 4. Fig. 8 depicts means of transport for evacuation. The percentage of people on foot is high in TZ3 El Morro, and TZ2 Central Talcahuano, while use of cars (4 to 7, both driving a car or pickup, and getting a car ride or a pickup ride) is higher in TZ4 Salinas, followed by DCH, Dichato. In this figure, 'other' refers to those who could not or did not evacuate and stayed in the buildings. Such cases represent a share of more than 30% in TZ2 Central Talcahuano, where 3-4 story apartments are common. Traffic jam conditions (Fig. 9) vs survey zones indicate similar patterns of severe conditions in TZ4 Salinas and Dichato.

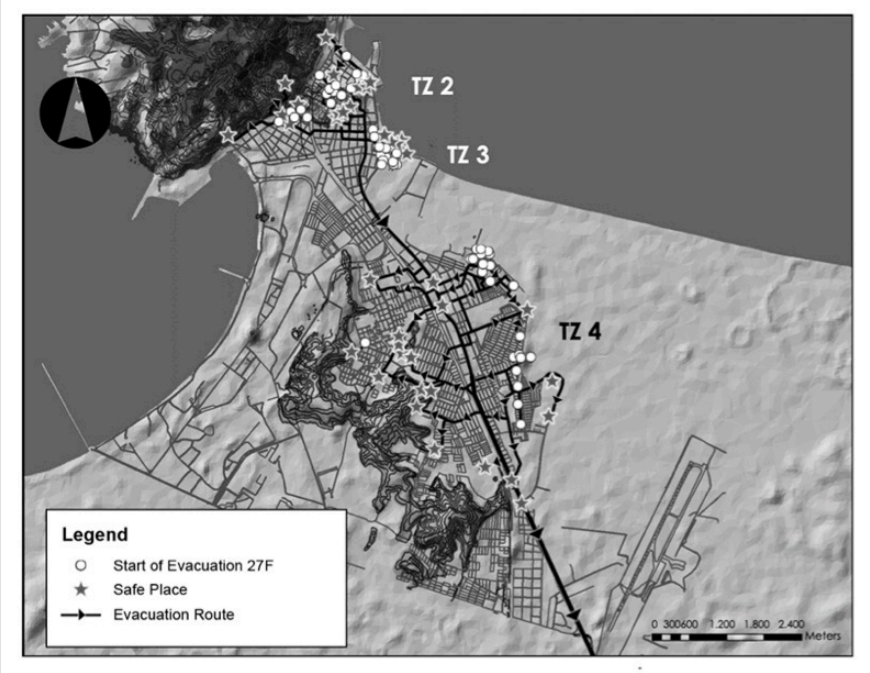

Fig. 6 Evacuation GIS map of 27F2010, in Talcahuano (Zone 2 is Central, Zone 3 is El Morro, and Zone 4 is Salinas). Circles are origins of evacuation and stars are destinations in safety zones.

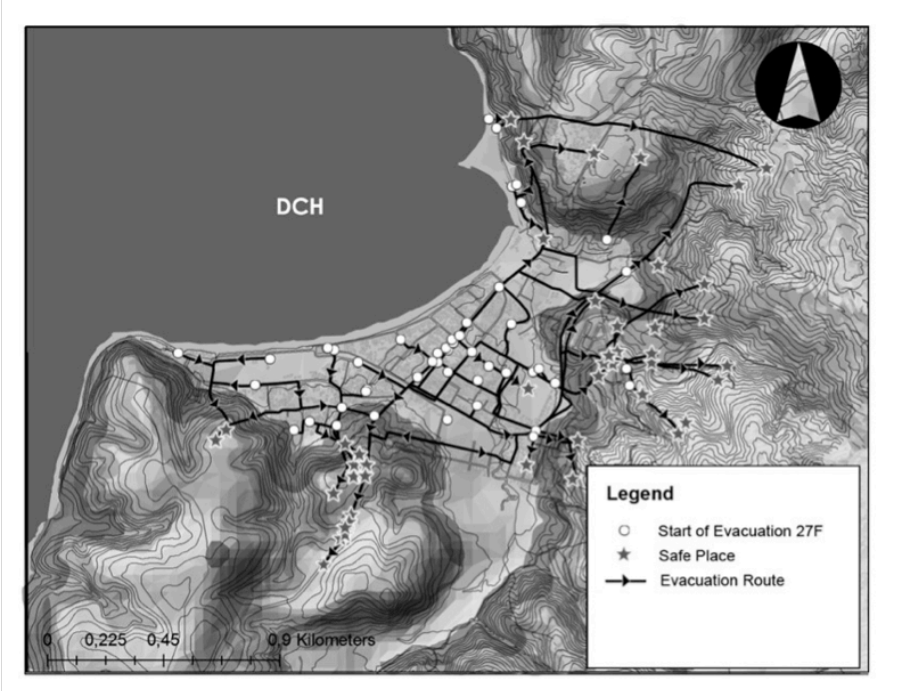

Fig. 7 EvacuationGIS map of 27F, 2010 in Dichato (DCH). Circles are origins of evacuation and stars are destinations in safety zones.

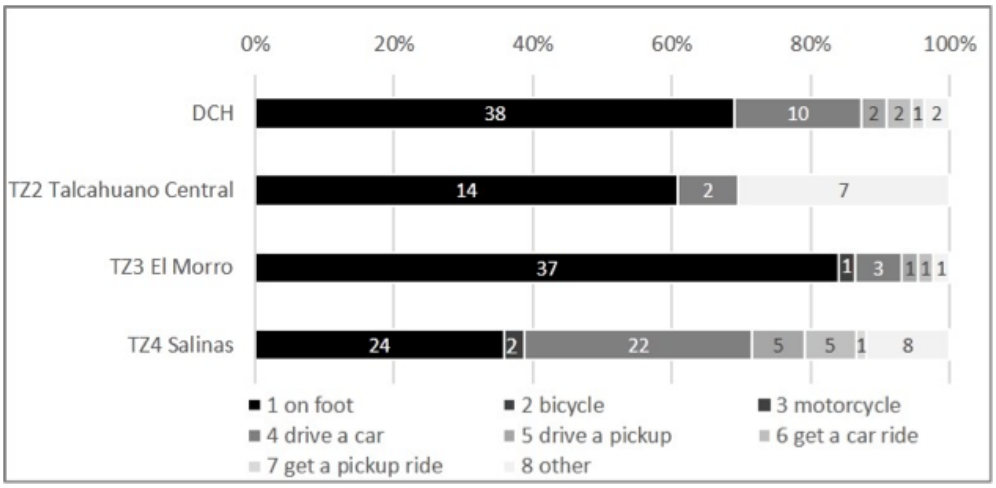

Fig. 8 Means of transport for evacuation vs. survey zones (Q6, n=189)

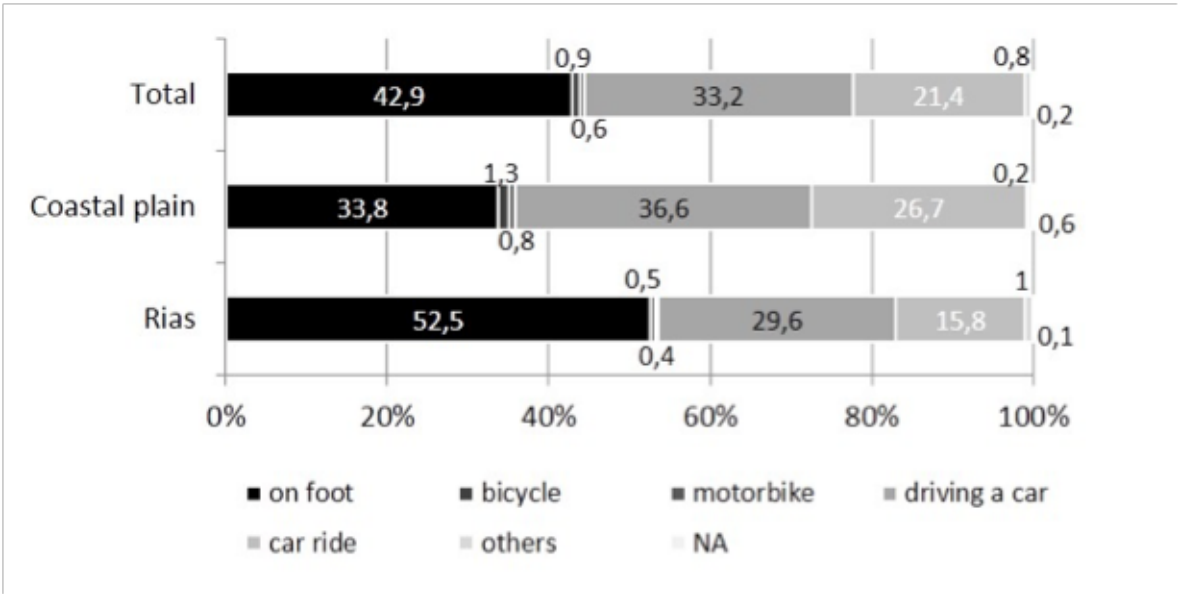

Fig. 9 Traffic jams observation vs. survey zones (Q14, n=186)

The reasons for predominant pedestrian evacuation in Talcahuno and Dichato are based on rules and morals, and people tend to consider it is safer to walk than to drive or ride a car. Fig. 10 shows mobility patterns in the 2011 Great Tohoku earthquake and tsunami. Automobile evacuation was higher in the coastal plain area than in Rias region, and automobile use in Tohoku was much higher than in Talcahuano and Dichato.

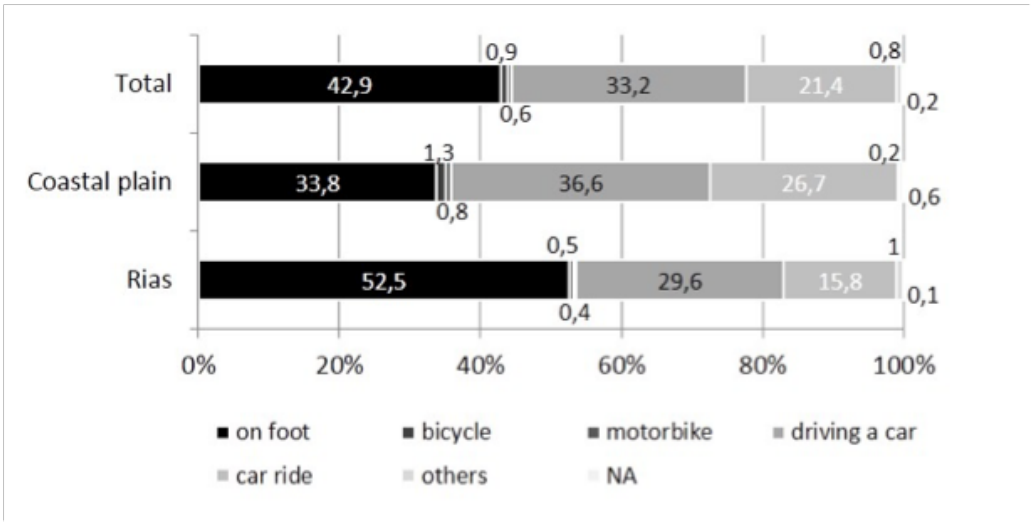

Fig. 10 Relation between means of transport for tsunami evacuation and regional topography in the 2011 Great Tohoku earthquake and tsunami (Fukko Shien survey archive, MLIT survey, n=5524 cases)

4.3 Conditions of evacuation routes, evacuation zones and universal access

Most people evacuated to safe areas just to walk in the nearby hills (Fig. 11). The evaluation of evacuation routes ranked 'bad' and 'very bad' in all areas where surveys were conducted (Fig. 12). This is mainly due to poor signage of the tsunami evacuation routes, or to routes being blocked by debris from the earthquake, or to lack of artificial lighting. Safe places are also classified as 'bad' because they do not have any basic facilities or services (bathrooms, drinking water, electricity, climate protection) to enable the sheltering of people.

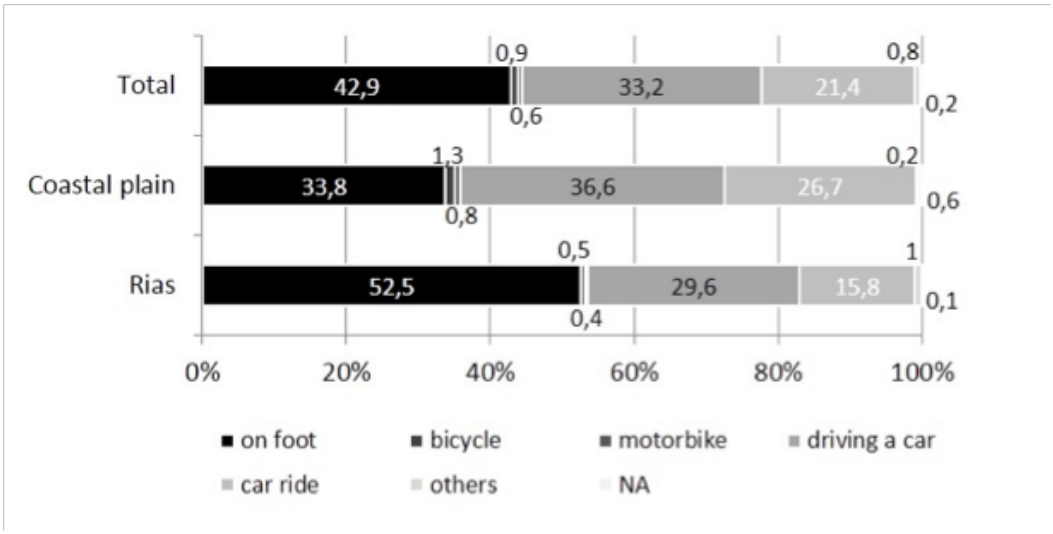

Fig. 11 Evacuation place vs. survey zones (Q10, n=187)

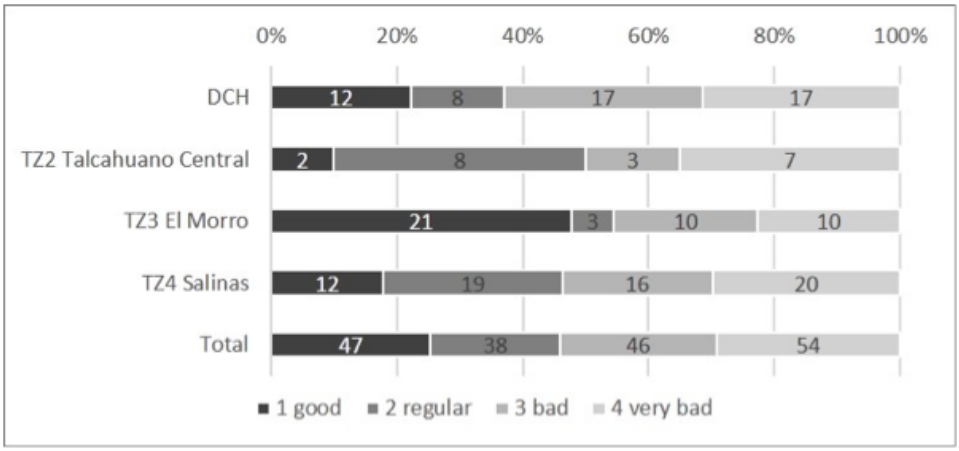

Fig. 12 Rating evacuation route vs. survey zones (Q13, n=185)

4.4 Assumption of a daytime earthquake on a weekday

The 2010 Maule earthquake occurred at night time at the weekend. As for the means for travelling, 40% do it on foot and 27% by buses or trains, while private car travellers are 11%. Supposing an earthquake should have occurred during day time of a week day, the means of transport and travelling patterns are of critical interest (Fig. 13). The daytime evacuation pattern is shown in Fig.13. Those who plan to go back home from work places are about 25%, and those who plan to go and see their family and then evacuate are about 10%. A day time earthquake and tsunami threat seems to increase two-way traffic going home, going to see family and then evacuating, though car use may not increase much in such cities, as the majority of commuters still use public transportation like buses and trains.

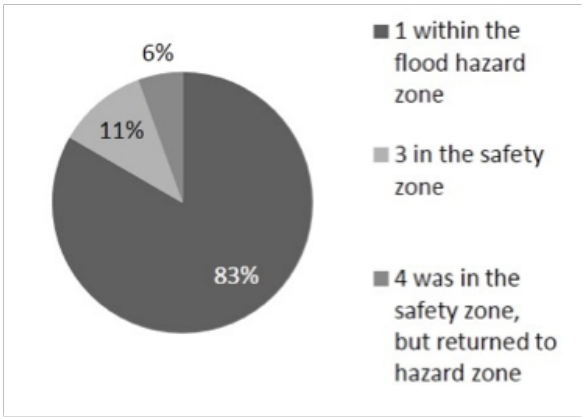

Fig. 13 Evacuation pattern assuming daytime earthquake vs. survey zones (Q24, n=191)

4.5 Summary of findings in the Biobío tsunami evacuation 2010

A questionnaire survey was conducted in Talcahuano and Dichato to investigate evacuation behavior after the 2010 Biobío Earthquake and subsequent tsunami.

1. Most of the people evacuated within 20 minutes after the earthquake, even though there was no official tsunami warning. However, about 30% of cases could not or did not evacuate in due time and stayed on the upper floors of apartment buildings or second floor of houses.
2. The majority (nearly 60%) of transportation for evacuation was on foot, while about 15% occurred by driving a car or a pickup, and getting a car or pickup ride. Use of cars for evacuation is much higher in TZ4 Salinas and in Dichato, and a correlation between the use of cars and evacuation distances is obvious. Traffic jams occurred more in Dichato and TZ4 Salinas than in TZ2 Central Talcahuano and TZ3 El Morro.
3. In case of a daytime earthquake, many think they would either go home or go to see their family before evacuating. Such behavior may increase demand for traffic and increase traffic jams and the difficulty of evacuation.
4. Family education on tsunamis and evacuation tends to increase the percentage of respondents who evacuate quickly.

5 Questionnaire on tsunami evacuation for the 2015 Coquimbo earthquake in the city of Talcahuano.

5.1 Perception of risk after the evacuation alarm and evacuation start time

In order to elucidate the behavior of inhabitants during the tsunami evacuation in Talcahuano for the 2015 Coquimbo earthquake, a survey was conducted during January 2015, with the help of students from the University of Concepción. The study areas are the same as for the 2010 tsunami study, TZ2 (Central Talcahuano), TZ3 (El Morro) and TZ4 (Salinas), aimed at comparing the behavior during the evacuation for the 2010and 2015 tsunamis in Talcahuano. A total of 58 data cases were collected. The results of the surveys for: tsunami warning, evacuation means, evacuation routes, and participation in evacuation drill are discussed here.

After the 2010 earthquake, Chile implemented a tsunami alarm system in the main coastal cities of the country, so in Talcahuano the authorities activated the sirens after the strong earthquake in 2015. Fig. 14 shows that 83% of the respondents were in the flood hazard zones, 11% in safe areas, and 6% said they had been in a safe area but returned to the hazard zone to see their relatives or protect their houses from thieves.

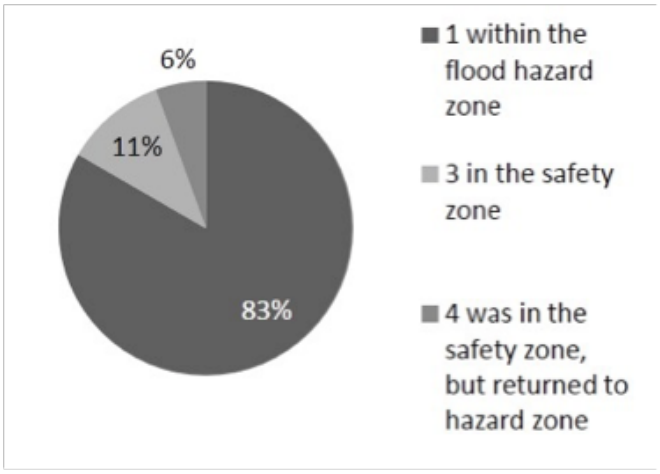

Fig. 14 Where were you when you heard siren (Q5B, n=58)

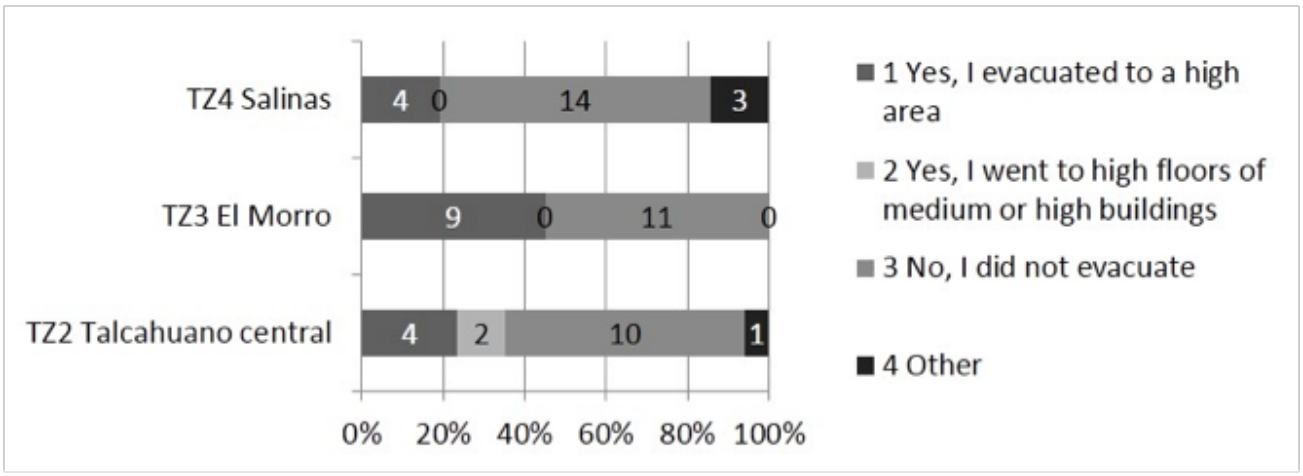

Fig. 15 Did you evacuate from tsunami (Q4, n=58)

Fig. 15 shows whether respondents evacuated to security zones or not, where 32% evacuated to high security areas and 68% said they did not evacuate, mainly because they considered that the earthquake was not strong enough compared to 27F in 2010, despite the fact that 72% reported having heard the evacuation siren (Fig. 16).

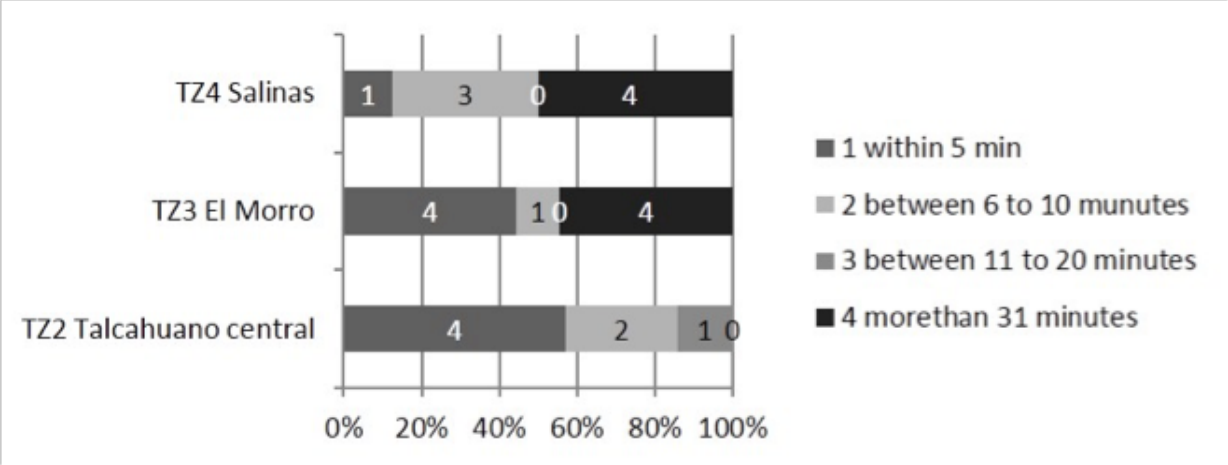

Fig 16 Did you hear tsunami alert or siren (Q5, n=58)

Of all respondents 38% evacuated 5 minutes after the earthquake, 25% between 6 and 10 minutes later and 33% after 31 minutes from the earthquake. In the TZ4 Salinas area, which is characterized by a flat area with distant hills, the slowest evacuation was recorded, where 50% evacuated to security zones between 5 and 10 minutes after the earthquake; meanwhile, in the TZ2 Central Talcahuano zone, the evacuation was the fastest, with 83% evacuated to high safety zones between 5 and 10 minutes after the earthquake (Fig. 17). Table 2 shows time taken to start evacuation in the 2011 Great Tohoku earthquake tsunami. It is clear that evacuation of Talcahuano in 2010 and 2015 is much faster.

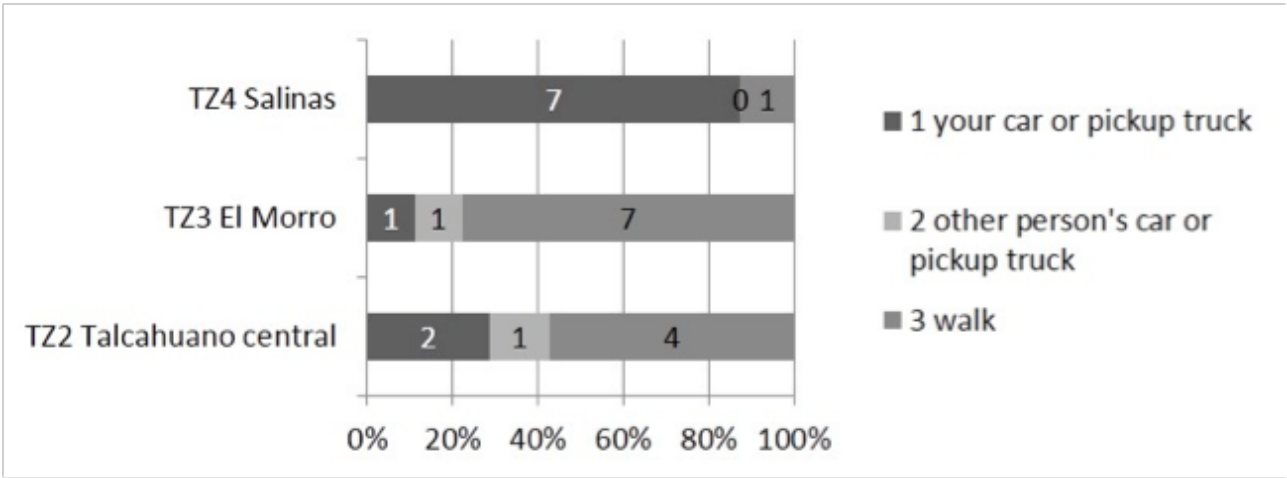

Fig. 17 When did you start to evacuate? (Q6B, n=58)

Table 2 Time taken to start evacuation in the 2011 Great Tohoku earthquake tsunami, by MLIT survey for disaster restoration (Murakami).

Tsunami risk perception after eq.	No. of cases	Average starting time after eq. (min.)	Time at which 50% of people started evacuation (min.)	Time at which 80% of people started evacuation (min.)
I thought tsunami should come, or I thought tsunami might come.	3105	18	14	29
I thought tsunami would noto come, or I didn't think about tsunami.	2411	25	24	42
Total	5524	22	14	34

5.2 Transport means for evacuation

Fig. 18 shows that in the TZ4 Salinas area, where the flattest topography is observed, 87% of people evacuated by cars or pickup trucks, mainly because the safety zones are defined in the hills, 2 kilometres away from residential areas, a distance which people avoid walking, despite the fact that during the evacuation of 2010 a high traffic jam was recorded on the escape routes in this area. In the case of the TZ2 Central Talcahuano and TZ3 El Morro areas, where the safe zones are defined in the hills that are less than 500m away, the evacuation was conducted mainly walking.

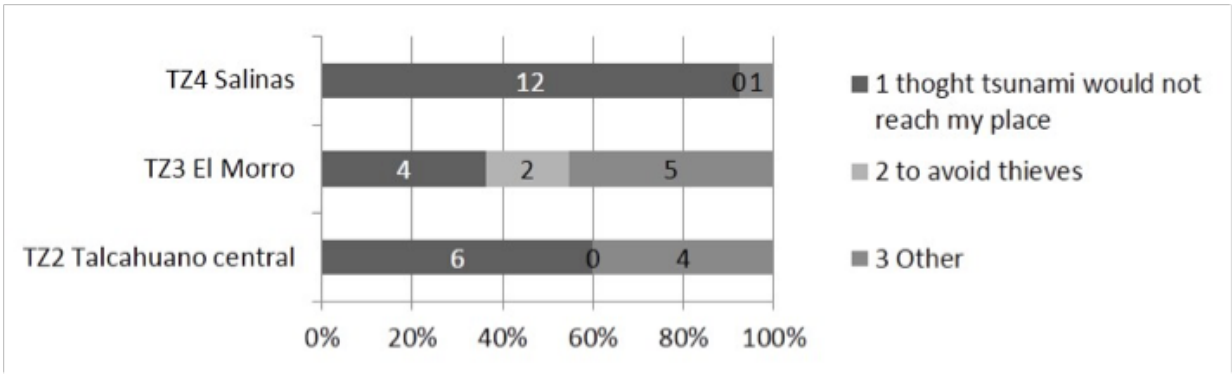

Fig. 18 Transport means to evacuate (Q6C, n=58)

Fig. 19 shows that people in the TZ4 Salinas area (where the flattest topography is observed and where safe hill areas are 2 km from point at the highest risk) did not evacuate because they thought the tsunami would not reach their houses, even though the evacuation alarm was activated. This shows the low perception of the risk by the population when comparing the smaller magnitude of the 2015 earthquake with that of 2010. Another factor that influenced the decision not to evacuate was to avoid leaving their homes alone for fear of thievery.

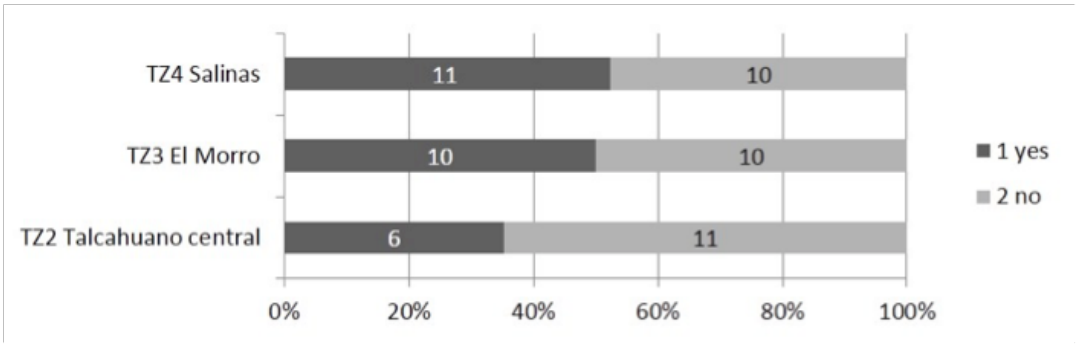

Fig. 19 Main reason you did not evacuate (Q7, n=58)

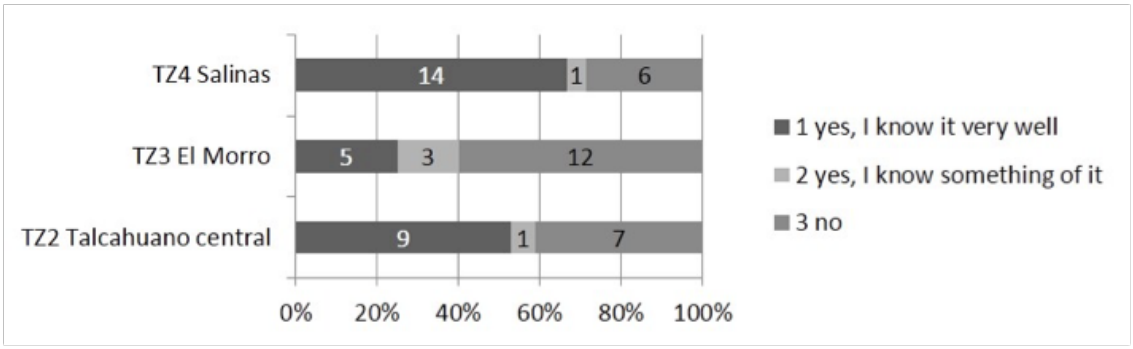

Fig. 20 Did you participate in tsunami evacuation drills? (Q10, n=58

Fig. 20 and Fig. 21 show that approximately 50% of people participated in evacuation drills and claimed to know the evacuation maps spread by the Municipality, which shows an interest in preparing for future emergencies.

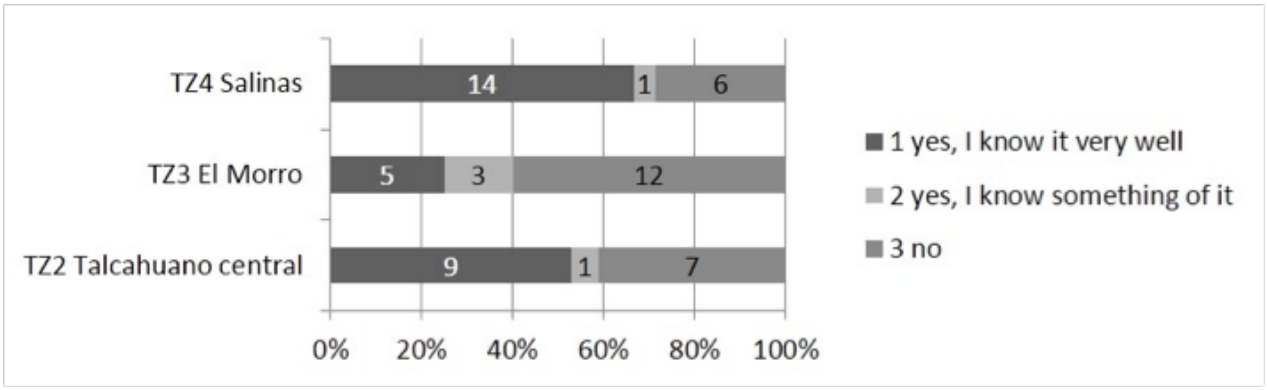

Fig. 21 Did you know the city tsunami risk map (Q22, n=58)

5.3 Summary of findings in the Talcahuano tsunami evacuation 2015

A questionnaire survey was conducted in Talcahuano to investigate evacuation behavior after the 2015 Coquimbo Earthquake and subsequent tsunami.

1. In relation to the 2015 earthquake, respondents point out that the perception of risk was lower than for the 2010 tsunami, despite the activation of the alarm for evacuation, which is reflected in the fact that only 32% of the respondents evacuated to high areas.
2. People from the TZ4 area evacuated the risk zone mainly by car, because of a greater distance to the safe areas, causing traffic jams in the evacuation routes, which triggered conflicts between the pedestrians and the car occupants. In the case of TZ2 and TZ3 areas, people evacuated mainly by walking to nearby hills, within 500 m distance.
3. After the 2010 earthquake, the Municipality of Talcahuano has constantly carried out tsunami evacuation drills where the population generally participate; this certainly helps to prepare for future events. However, the low percentage of evacuation during the 2015 tsunami alarm is mainly due to the low levels of perception of risk among the population, when compared to the great earthquake of 2010.
4. In general, families claim to know the tsunami risk maps, which helps to keep track of evacuation routes and safe areas to react in a timely manner. This contrasts with the perception of risk when people compare the lower magnitude of the 2015 earthquake with that of the 2010 disaster, not aware that a smaller magnitude earthquake can equally trigger a potentially disastrous tsunami.

6. Conclusions

The 2010 Maule earthquake and the 2015 off coast Coquimbo earthquake caused tsunami in Chile, and the questionnaire surveys were conducted in the cities of Talcahuano and Dichato, the most affected cities. This study analyzed and compared tsunami evacuation behavior and affecting factors in view of urban form and evacuation environments. The findings are as follows.

Tsunami evacuation tends to be faster in Chile than in Tohoku, however, it is important to address the fact that tsunami arrival times in Chile can be much faster than in Tohoku. An approximate 5% to 10% of people did not evacuate as they thought the tsunami would not affect their homes or they wanted to protect their homes from thieves. Besides, it is important to determine how to better support elderly and handicapped people for evacuation. Tsunami warning systems in Chile are developing fast and now people are getting more frequent warnings than before, in cases of smaller seismic activities. As for the means of transport, the majority of people evacuate on foot as they respect it as a basic rule. However, automobile evacuation tends to increase in areas where car ownership and daily use of automobiles are common, such as suburbs where evacuation places are far or in upper class communities. People evacuating on foot face various difficulties and risks due to traffic jams caused by automobiles or fast moving vehicles.

A difference is detected in the evacuation process between the areas of the city where hills are higher and closer and the flat sectors with distant hills; in the first areas, evacuation is faster and it is mainly on foot, unlike the second areas, where evacuation tends to be slower and the use of an automobile increases considerably, causing jams on the roads.

At the moment of the tsunami, evacuation routes in the cities of Talcahuano and Dichato were poorly signposted and 25% of people rated them as good, 21% as 'regular', and 54% as 'bad' and 'very bad'; this is mainly because their design did not facilitate the displacement of people and, after the earthquake, the roads were obstructed by debris that fell off the facades of buildings; similarly, the safe zones did not provide a minimum of facilities or services, such as drinking water, protection against the weather, or health services, making it difficult for people to remain in them.

The two earthquakes occurred at night time when family members were mostly at home and together. In cases of a daytime earthquake, people may try to get back home to help the elderly or children, at home or in nursing schools and such trips by automobiles increase traffic. Studies on working people and work places, such as industries and offices, with regards to tsunami evacuation are important as they improve protocols and awareness of tsunami related hazards.

In the case of the 2015 earthquake, in Talcahuano the evacuation rate of people away from the risk zone was low (32% evacuated to high areas), despite the fact that the tsunami alarm was activated. This was due to the low perception of risk among the population, because of the lower magnitude of this earthquake (8.4 Mw) compared to that of the 2010 earthquake (8.8 Mw). This behavior may constitute a false perception of risk considering that an 8.4 Mw magnitude earthquake can produce a potentially destructive tsunami.

Acknowledgements

The study was conducted for the research project in Chile entitled "Enhancement of Technology to Develop Tsunami-Resilient Communities", which was headed by Dr. T. Tomita of Port and Airport Research Institute, supported by JST/JICA SATREPS in collaboration with Chilean researchers and counterparts. The authors acknowledge inhabitants of Talcahuano and Dichato, who kindly answered questionnaires, JICA Chile office and the project coordinators who continuously supported our field work in Biobío. The authors express sincere gratitude to the students of the University of Concepción who participated in the survey, Ms. Alejandra Contreras, and Mr. Patricio Diaz who assisted the study by GIS mapping of evacuation routes, and Prof. Edilia Jaque who kindly provided us with GIS base map data.

References

Ayala, F and Olcina, J.,2002. Riesgos naturales. Barcelona: Ariel.

Boisier, S., 2001. Desarrollo local: ¿De qué estamos hablando ? Transformaciones globales. Instituciones y politicas de desarrollo local, pp. 48-74. Rosario: Homo Sapiens.

Fraser, S., Graham, L., Murakami,H., and Matsuo, I., 2012. Tsunami Vertical Evacuation Buildings- Lessons for international Preparedness Following the 2011 Great East Japan tsunami, Journal of Disaster Research Vol. 7 No.sp, 2012.

Gusiakov, V. K., 2005. Tsunami generation potential of different tsunamigenic regions in the Pacific. Marine Geology, 215 (1-2): 3-9.

Imamura, F. U., Bernard, E. N. and Robinson, A., 2009. Tsunami modeling: calculating inundation and hazard maps. The sea, 15: 321-332.

Kastenberg, W.E., 2015. Ethics, risk, and safety culture: reflections on Fukushima and beyond. Journal of Risk Research, 18 (3): 304-316.

Kelleher, J. A., 1972. Ruptures zones of large South American earthquakes and some predictions. Journal of Geophysical Research, 77 (11): 2087-2103.Kontar, Y. A., Santiago-Fandiño, V. and Takahashi, T. (2014). Tsunami Events and Lessons Learned. Springer Netherlands: 467 pp.

Liu, Y., Santos, A., Wang, S.M., Shi, Y., Liu, H. and Yuen, D.A., 2007. Tsunami hazards along Chinese coast from potential earthquakes in South China Sea. Physics of the earth and planetary interiors, 163(1): 233-244.

Maruyama, Y., S. Matsuzaki, F. Yamazaki, H. Miura and M. Estrada, 2010. Development of GIS dataset for damage distribution analysis after the 2010 Chile Earthquake, Journal of Japan Society of Civil Engineers, A1, Vol. 66, No.1, pp.377-385.

Murakami, H., Ramos, L., 2014. Tsunami evacuation questionnaire survey for cities of Talcahuano and Dichato in the 2010 Maule earthquake in Chile, Part 2 Survey results, Proc. 14th Japan Earthquake Engineering Symposium, paper number OS13-Fri-AM-3.

Murakami, H., Nagase, Y., Takahashi, M., Asai, K., Ikeda, M., and Sase, K., 2015. Study on Tsunami Evacuation after the 2014 Iquique Earthquake, Chile (2) Results of Questionnaire Survey for Inhabitants, Proc. Annual Research Meeting, Chugoku Chapter, Architectural Institute of Japan, No. 38.

Murakami, H. and Okumura, Y., 2014. Study on Tsunami Evacuation after the 2014 Iquique Earthquake, Chile (1) Hearing Survey for Public Offices, Communities, and Shopping Center, Proc. Annual Research Meeting, Chugoku Chapter, Architectural Institute of Japan.

Pujadas, R. y Font, J., 1998. Ordenacion y planificacion territorial. Madrid: Síntesis.

Ramos, L., and Murakami H., 2014. Tsunami evacuation questionnaire survey for cities of Talcahuano and Dichato in the 2010 Maule earthquake in Chile Part 1 Background and survey scheme, Proc. 14th Japan Earthquake Engineering Symposium, paper number OS13-Fri-AM-2.

Ramos, L., 2016. Urban Evacuation Tsunamis: Guidelines for Urban Design. Journal of Engineering and Architecture, Vol. 4, No. 2, pp. 117-132.

Saito, T., Ito, Y., Inazu, D. and Hino, R., 2011. Tsunami source of the 2011 Tohoku‐Oki earthquake, Japan: Inversion analysis based on dispersive tsunami simulations. Geophysical Research Letters, 38 (7): 1-5.

Serra, A., 2011. Turning hazards into resources? Floods, wetlands and climate change in Mediterranean coast of Spain. (Tesis doctoral), Universidad Autonoma de Barcelona, Barcelona.

Tomita, T., Kumagai, K., Mokurani, C., Cienfuegos, R., and Matsui, H., 2014. Post field survey on the April 2014 Earthquake and Tsunami in Northern Chile, Proc. 14th Japan Earthquake Engineering Symposium, paper number OS12-Fri-AM-4.

Wilches- Chaux, G., 1993. La vulnerabilidad gloval. Los desastres no son naturales, pp. 11-44: La Red.

Zilbert, L., 2010. Evolución de las políticas de la reducción de riesgo de desastres. En PNUD (Ed.), Diplomado de Especialización en Desarrollo Local y Gestión Integral del Riesgo (hoja de ruta) PNUD: escuela virtual.

ISSN 8755-6839

SCIENCE OF TSUNAMI HAZARDS

Journal of Tsunami Society International

Volume 38 Number 1 2019

TSUNAMI SOCIETY INTERNATIONAL, 1741 Ala Moana Blvd. #70, Honolulu, HI 96815, USA.

WWW.TSUNAMISOCIETY.ORG

ISSN 8755-6839

SCIENCE OF TSUNAMI HAZARDS

Journal of Tsunami Society International

Volume 38 Number 1 2019

TSUNAMI SOCIETY INTERNATIONAL, 1741 Ala Moana Blvd. #70, Honolulu, HI 96815, USA.

WWW.TSUNAMISOCIETY.ORG